C

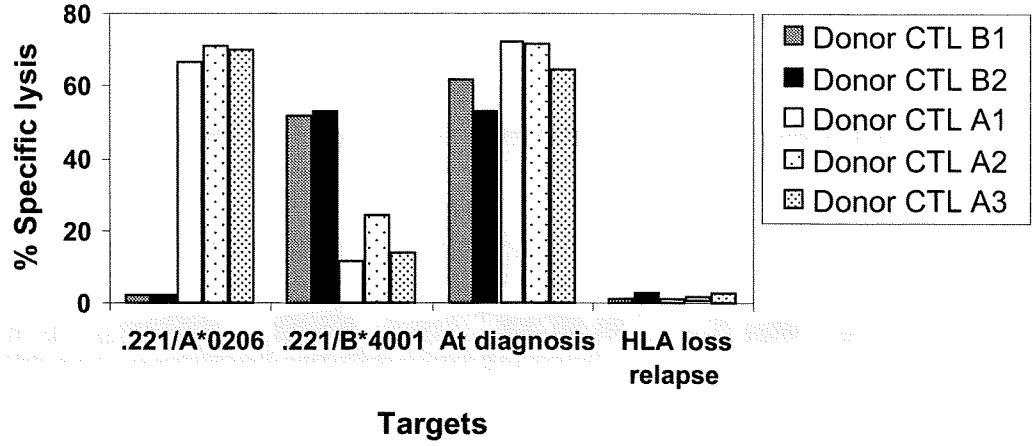
80
60
40
20
0
% Specific lysis
Donor CTL B1
Donor CTL B2
Donor CTL A1
Donor CTL A2
Donor CTL A3
.221/A*0206
.221/B*4001
At diagnosis
HLA loss relapse
Targets

D

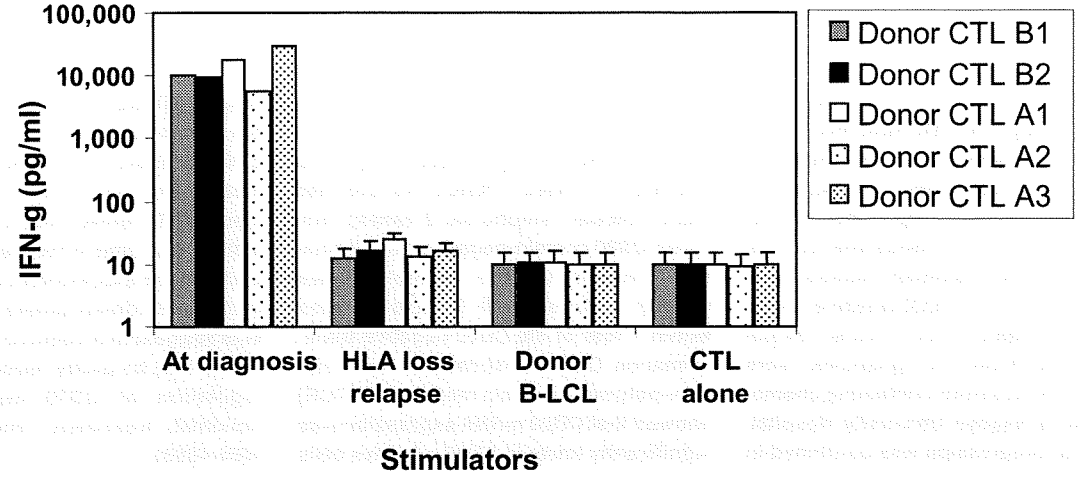
100,000
10,000
1,000
100
10
1
IFN-g (pg/ml)
Donor CTL B1
Donor CTL B2
Donor CTL A1
Donor CTL A2
Donor CTL A3
At diagnosis
HLA loss relapse
Donor B-LCL
CTL alone
Stimulators

Down-regulation of CD20 expression in B-cell lymphoma cells after treatment with rituximab-containing combination chemotherapies: its prevalence and clinical significance

Junji Hiraga,[1,2] Akihiro Tomita,[1] Takumi Sugimoto,[1] Kazuyuki Shimada,[1] Masafumi Ito,[3] Shigeo Nakamura,[4] Hitoshi Kiyoi,[5] Tomohiro Kinoshita,[1] and Tomoki Naoe[1]

[1]Department of Hematology and Oncology, Nagoya University Graduate School of Medicine, Nagoya; [2]Department of Hematology, Toyota Memorial Hospital, Toyota; [3]Department of Pathology, Japanese Red Cross, Nagoya First Hospital, Nagoya; [4]Department of Pathology and Clinical Laboratories, Nagoya University Hospital, Nagoya; and [5]Department of Infectious Diseases, Nagoya University School of Medicine, Nagoya, Japan

Although rituximab is a key molecular targeting drug for CD20-positive B-cell lymphomas, resistance to rituximab has recently been recognized as a considerable problem. Here, we report that a CD20-negative phenotypic change after chemotherapies with rituximab occurs in a certain number of CD20-positive B-cell lymphoma patients. For 5 years, 124 patients with B-cell malignancies were treated with rituximab-containing chemotherapies in Nagoya University Hospital. Relapse or progression was confirmed in 36 patients (29.0%), and a rebiopsy was performed in 19 patients. Of those 19, 5 (26.3%; diffuse large B-cell lymphoma [DLBCL], 3 cases; DLBCL transformed from follicular lymphoma, 2 cases) indicated CD20 protein-negative transformation. Despite salvage chemotherapies without rituximab, all 5 patients died within 1 year of the CD20-negative transformation. Quantitative reverse-transcription–polymerase chain reaction (RT-PCR) showed that CD20 mRNA expression was significantly lower in CD20-negative cells than in CD20-positive cells obtained from the same patient. Interestingly, when CD20-negative cells were treated with 5-aza-2′-deoxycytidine in vitro, the expression of CD20 mRNA was stimulated within 3 days, resulting in the restoration of both cell surface expression of the CD20 protein and rituximab sensitivity. These findings suggest that some epigenetic mechanisms may be partly related to the down-regulation of CD20 expression after rituximab treatment. (Blood. 2009;113: 4885-4893)

Introduction

Rituximab is a murine/human chimeric anti-CD20 monoclonal antibody that has become a key molecular targeting drug for CD20-positive B-cell lymphomas.[1,2] Many favorable results using combination chemotherapy with rituximab for both CD20-positive de novo and relapsed low-grade and aggressive B-cell non-Hodgkin lymphoma have been reported in recent years.[3-7] In Japan, rituximab has also been used since September 2001 for patients with follicular lymphoma (FL), indolent lymphoma, and mantle cell lymphoma (MCL). In addition, since September 2003 in Japan, indications for using rituximab were expanded to include diffuse large B-cell lymphoma (DLBCL), further demonstrating the significant effectiveness of rituximab for B-cell lymphoma compared with conventional chemotherapies without rituximab.[8]

Although combination chemotherapies with rituximab have provided significantly favorable results for CD20-positive B-cell lymphoma patients, acquired resistance to rituximab has become a considerable problem. Several mechanisms of resistance were predicted as reported previously, including loss of CD20 expression, inhibition of antibody binding, antibody metabolism, expression of complement inhibitors such as CD55/CD59, and membrane/lipid raft abnormality (reviewed by Smith et al[9]),[10-19] but the clinical significance of those mechanisms has remained unclear. In the last 5 years, a CD20-negative phenotypic change in CD20-positive lymphomas after rituximab treatment has been reported by several groups,[16,20-31] indicating that this phenomenon after the use of rituximab may not be rare. Although these reports contain important information from clinical experiences, the frequency of occurrence and detailed molecular biologic information about the CD20-negative phenotype remain to be elucidated.

Very recently, we reported a CD20-negative DLBCL case that had transformed from CD20-positive FL after repeated treatment with rituximab. We established an RRBL1 cell line from this patient,[32] and the mechanisms of the CD20-negative change were analyzed in these cells. CD20 mRNA expression was significantly lower than in CD20-positive cells, resulting in a loss of CD20 protein expression as detected by flow cytometry (FCM), immunohistochemistry (IHC), and immunoblotting (IB). Interestingly, trichostatin A (TSA), a histone deacetylase inhibitor, was able to successfully stimulate CD20 expression, suggesting that some epigenetic mechanisms may have repressed the expression. Thus, an accumulation of detailed clinical and molecular biologic features is required to demonstrate the significance of CD20-negative phenotypic changes after rituximab treatment.

In the last 5 years, 124 patients with CD20-positive B-cell malignancies received chemotherapy with rituximab at Nagoya University Hospital, 36 (29.0%) of whom showed relapse/progression. Among these 36 patients, CD20 protein-negative or -decreased phenotypic changes were confirmed in 5 cases concomitant with disease progression. Here, we describe the occurrence rate of CD20-negative transformation after rituximab treatment, as well

Submitted August 19, 2008; accepted February 25, 2009. Prepublished online as *Blood* First Edition paper, February 26, 2009; DOI 10.1182/blood-2008-08-175208.

The online version of this article contains a data supplement.

The publication costs of this article were defrayed in part by page charge payment. Therefore, and solely to indicate this fact, this article is hereby marked "advertisement" in accordance with 18 USC section 1734.

Table 1. CD20-positive B-cell malignancies treated with rituximab in Nagoya University Hospital

	No. of patients	Disease status at rituximab therapy		Response, RD/PD	Resampling of tumor tissue	CD20 expression, +/±/−
		1st	RD/PD			
DLBCL	51	45	6	13	6	3/1/2
FL	43	26	17	13	7	5/0/2
Nodal marginal zone BCL or MALT	8	6	2	2	2	2/0/0
Burkitt or Burkitt-like	5	5	0	4	2	2/0/0
Mediastinal large B-cell	4	2	2	1	0	0
Intravascular large B-cell	4	4	0	2	1	1/0/0
Mantle cell	4	3	1	1	1	1/0/0
Lymphoplasmacytic	3	3	0	0	0	0
CLL/SLL	2	1	1	0	0	0
Total cases	124	96	28	36	19	14/1/4
Probability (%)				36/124 (29.0)	19/36 (52.5)	5/19 (26.3)

DLBCL indicates diffuse large B-cell lymphoma; FL, follicular lymphoma; BCL, B-cell lymphoma; MALT, mucosa-associated lymphoid tissue; CLL/SLL, clonic lymphocytic leukemia/small lymphocytic lymphoma; 1st, the first treatment; RD/PD, relapse or progression; and +/±/−; positive/decreased/negative.

as the molecular background of the CD20 protein-negative phenotype in cells from those patients.

Methods

Patients

Between February 1988 and November 2006 in Nagoya University Hospital, all 124 patients in this analysis were initially diagnosed with CD20-positive B-cell lymphomas (Table 1) according to the World Health Organization (WHO) classification.[33] All patients were treated with combination chemotherapy with rituximab from September 2001 to December 2006. The median age of the patients was 58 years (range, 16-84 years) at the time of initial rituximab administration. Three patients had received rituximab before September 2001 because of their participation in a previous clinical study. The most recent follow-up date was July 31, 2007, and disease status factors such as relapse, recurrence, and progression were determined by clinical findings and diagnostic imaging using x-ray, computed tomography (CT), magnetic resonance imaging (MRI), and ^{18}F-fluorodeoxyglucose positron emission tomography (FDG-PET). Resampling of tumors at the time of relapse/progression and pathologic analysis of 19 patients was performed. The patients' responses to chemotherapies were evaluated using the International Working Group criteria.[34]

Confirmation of CD20 protein expression by IHC and FCM analyses

These studies were conducted with institutional review board approval from the Nagoya University School of Medicine. After obtaining appropriate informed consent from each patient, in accordance with the Declaration of Helsinki, tumor specimens were harvested from lymph nodes, bone marrow, peripheral blood, or spinal fluid. CD20 protein expression was demonstrated by IHC and/or FCM as indicated previously.[32,35] Briefly, we used mouse anti-CD20 (L26; Dako, Carpinteria, CA), anti-CD10 (Novocastra Laboratories, Newcastle-upon-Tyne, United Kingdom), and anti-CD79a monoclonal antibodies (Dako) for IHC, and mouse anti-CD20 (B2E9; Beckman Coulter, Fullerton, CA) and anti-CD19 (HD37; Dako) monoclonal antibodies for FCM. The CD79a antigen is a pan–B-cell marker that forms a B-cell receptor (BCR) protein complex. The percentages of negative and positive cells from FCM were determined from the data using an isotypic control antibody (mouse IgG1; Beckman Coulter).

Sequence analysis of the *MS4A1* (*CD20*) gene

Genomic DNA from tumor cells was extracted with a QIAamp DNA Blood Mini Kit (QIAGEN, Valencia, CA) and used for further polymerase chain reactions (PCRs). When sufficient tumor cells could not be obtained at diagnosis, genomic DNA from paraffin sections was extracted using the MagneSil Genomic, Fixed Tissue System (Promega, Madison, WI). Genomic DNA PCR was performed using AmpliTaq Gold (Applied Biosystems, Foster City, CA) to acquire fragments of the coding sequences of exons 3 to 8 of the *MS4A1* (*CD20*) gene. The following primers were designed from the appropriate intron sequences to achieve the coding sequences: exon 3-upper (U), 5′-GCT CTT CCT AAA CAA CCC CT-3′; exon 3-lower (L), 5′-CAT GGG ATG GAA GGC AAC TGA C-3′; exon 4-U, 5′-TGC TGC CTC TGT TCT CTC CC-3′; exon 4-L, 5′-CTG CAC CAT TTC CCA AAT GGC T-3′; exon 5-U, 5′-CTC CAT CTC CCC CAC CTC TC-3′; exon 5-L, 5′-GGT ACT TCT CTG ACA TGT GGG A-3′; exon 6-U, 5′-TGG AAT TCC CTC CCA GAT TAT G-3′; exon 6-L, 5′-CCT GGA GAG AAA TCC AAT CTC A-3′; exon 7-U, 5′-GTC TCC TGT ACT AGC AGT TC-3′; exon 7-L, GGC TAC TAC TTA CAG ATT TGG G-3′; exon 8-U, 5′-TGG TCA ATG TCT GCT GCC CT-3′; and exon 8-L, 5′-GCG TAT GTG CAG AGT ACC TCA AG-3′. Amplified fragments were cloned into a pGEM-T Easy Vector (Promega) and were sequenced using a DNA auto sequencer (ABI PRISM 310; Applied Biosystems). PCR fragments that contained each exon sequence were cloned into the pGEM-T vector, and at least 10 clones were sequenced. If a mutation was observed in 2 different clones, we verified that the sequence reflected a mutation in the tumor rather than a PCR error.

RNA extraction and reverse-transcription–polymerase chain reaction

A blood RNA extraction kit (QIAGEN) was used to isolate total RNA from tumor cells. cDNA was prepared as reported previously.[36] For reverse-transcription–polymerase chain reaction (RT-PCR) analyses of CD10, CD19, CD20, and β-actin, the following primers were designed: CD10-U, 5′-TTG TCC TGC TCC TCA CCA TC-3′; CD10-L, 5′-GTT CTC CAC CTC TGC TAT CA-3′; CD19-U, 5′-GAA GAG GGA GAT AAC GCT GT-3′; CD19-L, 5′-CTG CCC TCC ACA TTG ACT G-3′; CD20-U, 5′-ATG AAA GGC CCT ATT GCT ATG-3′; CD20-L, 5′-GCT GGT TCA CAG TTG TAT ATG-3′; β-actin-U, 5′-TCA CTC AAG ATC CTC A-3′; and β-actin-L, 5′-TTC GTG GAT GCC ACA GGA C-3′. Semiquantitative RT-PCR with AmpliTaq Gold was performed as described previously.[32] Quantitative RT-PCR was carried out using TaqMan PCR (ABI PRISM 7000; Applied Biosystems) as previously described.[32,36]

Immunoblot analysis

Cells (~5×10^5) were lysed in 100 μL lysis buffer (50 mM tris(hydroxymethyl)aminomethane [Tris]-HCl [pH 8.0], 1.5 mM $MgCl_2$, 1 mM ethylene glycol-bis(β-aminoethyl ester)-*N,N,N′,N′*-tetraacetic acid [EGTA], 5 mM KCl, 10% glycerol, 0.5% Nonidet P-40 [NP-40], 300 mM NaCl, 0.2 mM phenylmethylsulfonyl fluoride [PMSF], 1 mM dithiothreitol [DTT], and a Complete Mini protease inhibitor tablet [Roche Applied Science, Indianapolis, IN]). After centrifugation at 10 000*g* for 10 minutes, the supernatants were placed in new tubes and 100 μL of 2× sodium dodecyl sulfate (SDS) sample buffer was added. After boiling for 5 minutes, samples were

Table 2. CD20-negative RD/PD after treatment with rituximab-containing combination chemotherapy

UPN	Age/ sex	Diagnosis on admission	Status	Chemo Regimen	Total ritux	Duration until CD20⁻	Diagnosis (RD/PD)	Patho source	CD20 expression FCM	IHC	RT	CDS mutation	Survival after CD20⁻
1	65/M	DLBCL	2 rel	R-salvage	8	2M	DLBCL	BM	–	–	N.A.	S97F [2/16]	6M†
2	37/ F	DLBCL	1 diag	R-CHOP	8	9M	DLBCL	BM	±*	±†	N.A.	V247I [2/10]	4M†
3	75/M	DLBCL	1 diag	R-CHOP	7	10M	DLBCL	BM, CF	–	–	↓	WT	11M†
4	42/M	FL G1	2 rel	R-CHOP	4	23M	DLBCL	BM	–	–	↓	WT	11M†
5	52/M	FL G2	3 rel	R-cMOPP	14	81M	DLBCL	BM, LN‡	–	–	↓	WT	8M†

Status indicates disease status of those patients at the first treatment with rituximab; rel, relapse; duration until CD20−, duration (in months) until CD20− relapse or PD from the first rituximab treatment; total ritux, total times of rituximab treatment; patho source, sources of tumor tissues for pathologic analysis; BM, bone marrow; CF, cerebral fluid; LN, lymph node; RT, RT-PCR; N.A., not available; ↓, down-regulated; CDS, coding sequences; and survival after CD20−, duration from CD20-negative change until death.

*19% of tumor cells were $CD20^+$.

†30% of tumor cells showed $CD20^+$.

‡Lymph node sample obtained at autopsy.

separated by SDS–polyacrylamide gel electrophoresis (PAGE). Immunoblotting was carried out as described previously[32,37] using goat polyclonal anti-CD20 antibody (Santa Cruz Biotechnology, Santa Cruz, CA) and rabbit polyclonal anti-actin antibody (Santa Cruz Biotechnology).

Treatment of RRBL1 cells and primary lymphoma cells with the epigenetic drug 5-aza-2′-deoxycytidine

RRBL1[32] and primary lymphoma cells (5×10^5) were cultured in 6-well dishes in RPMI 1640 medium containing 10% fetal bovine serum (FBS) for 24 hours with or without 5-aza-2′-deoxycytidine (5-Aza; Sigma-Aldrich, St Louis, MO) at a final concentration of 100 mM. The cells were then washed twice with RPMI 1640 medium containing 10% FBS, and incubated for more than 2 days in the same medium without 5-Aza. Cells were harvested and used for total RNA and protein extraction.

Antibody-dependent cell-mediated cytotoxicity assay in vitro

Antibody-dependent cell-mediated cytotoxicity (ADCC) activity was analyzed by an in vitro chromium-51 (^{51}Cr) release assay. Target cells (RRBL1, Daudi, DHL10) were cultured in appropriate medium supplemented with 10% to 20% FBS. Each cell line (2.0×10^5 cells) was labeled with 100 μCI (3.7 MBq) of $Na_2{}^{51}CrO_4$ (PerkinElmer Japan, Tokyo, Japan) at 37°C for 1 hour. Human peripheral blood mononuclear cells (PBMC), which were obtained from a healthy donor, were prepared as effector cells of the cell-mediated cytotoxicity assay. ^{51}Cr-labeled target cells were divided into aliquots in 96-well plates (10^4 cells/well). Effector PBMC cells (5×10^5 cells/well) were then added to each well in the presence or absence of rituximab (0 to 31.25 μg/mL) and incubated for 4 hours at 37°C. Supernatants were obtained after a brief centrifugation and measured on a γ-ray counter (PerkinElmer). ^{51}Cr-labeled target cells without antibodies were lysed completely by NP-40 (2% final concentration) and used as a positive control (the maximal ^{51}Cr release). The percentage of lysed cells was calculated using the following formula: % cell lysis = [(experimental release (cpm) − background (cpm)/(maximal release (cpm) − background (cpm))] × 100%, where cpm indicates counts per minute.

Results

CD20-negative phenotypic change after treatment with rituximab

A total of 124 patients with CD20-positive B-cell malignancies were treated with rituximab-combined chemotherapy from September 2001 to December 2006 (Table 1). All patients were diagnosed with CD20-positive B-cell lymphomas by IHC and/or FCM analyses using their tumor tissue specimens. Thirty-six patients (29.0%) showed relapse and progression (response; relapse/progression of disease [RD/PD] in Table 1) of their disease after or during chemotherapies with rituximab. Tumor cells from 19 of these 36 patients (52.8%) were resampled at the time of RD/PD, and CD20 protein expression was analyzed by IHC and/or FCM. CD20 protein expression was not detected or was significantly decreased in 5 patients (DLBCL, 3 patients; FL, 2 patients). Therefore, in 26.3% of patients whose tumor cells were resampled at the time of RD/PD, a CD20-negative phenotypic transformation after rituximab treatment was observed.

Clinical and laboratory features of patients with a CD20-negative phenotypic change

The clinical features of the 5 patients with a CD20-negative phenotypic change after rituximab treatment are shown in Table 2. Initially, 3 patients were diagnosed with DLBCL and 2 patients were diagnosed with FL. They were treated with chemotherapy with rituximab (375 mg/m^2) repeatedly until a CD20-negative phenotypic change was observed. Four to 14 cycles of rituximab were administered. These 5 patients showed relapse or progression from 2 to 81 months after their first treatment with rituximab. Histologic transformation from FL was observed in 2 patients, resulting in all 5 patients being diagnosed histologically as DLBCL at the time of RD/PD. Tumor cell infiltration into the bone marrow was observed in all 5 patients. A CD20 protein-negative phenotype was confirmed by IHC (Figure 1) and FCM in all 5 cases. In 3 patients, mRNA from tumor tissues was available, and CD20 mRNA expression was faintly observed using RT-PCR. Although all 5 patients received salvage chemotherapy without rituximab, they all died from disease progression within 11 months of the confirmation of CD20-negative transformation. The clinical outcomes of these patients who showed RD/PD after treatment with rituximab-containing chemotherapy are shown in Table 3. The 5 patients with CD20-negative RD/PD tended to have a shorter survival time than with CD20-positive RD/PD (100% vs 35.7% died). However, statistical significance could not be determined because of the variable disease status of each patient, including different backgrounds, salvage chemotherapies, and other factors. More patients must be studied to further analyze this apparent trend.

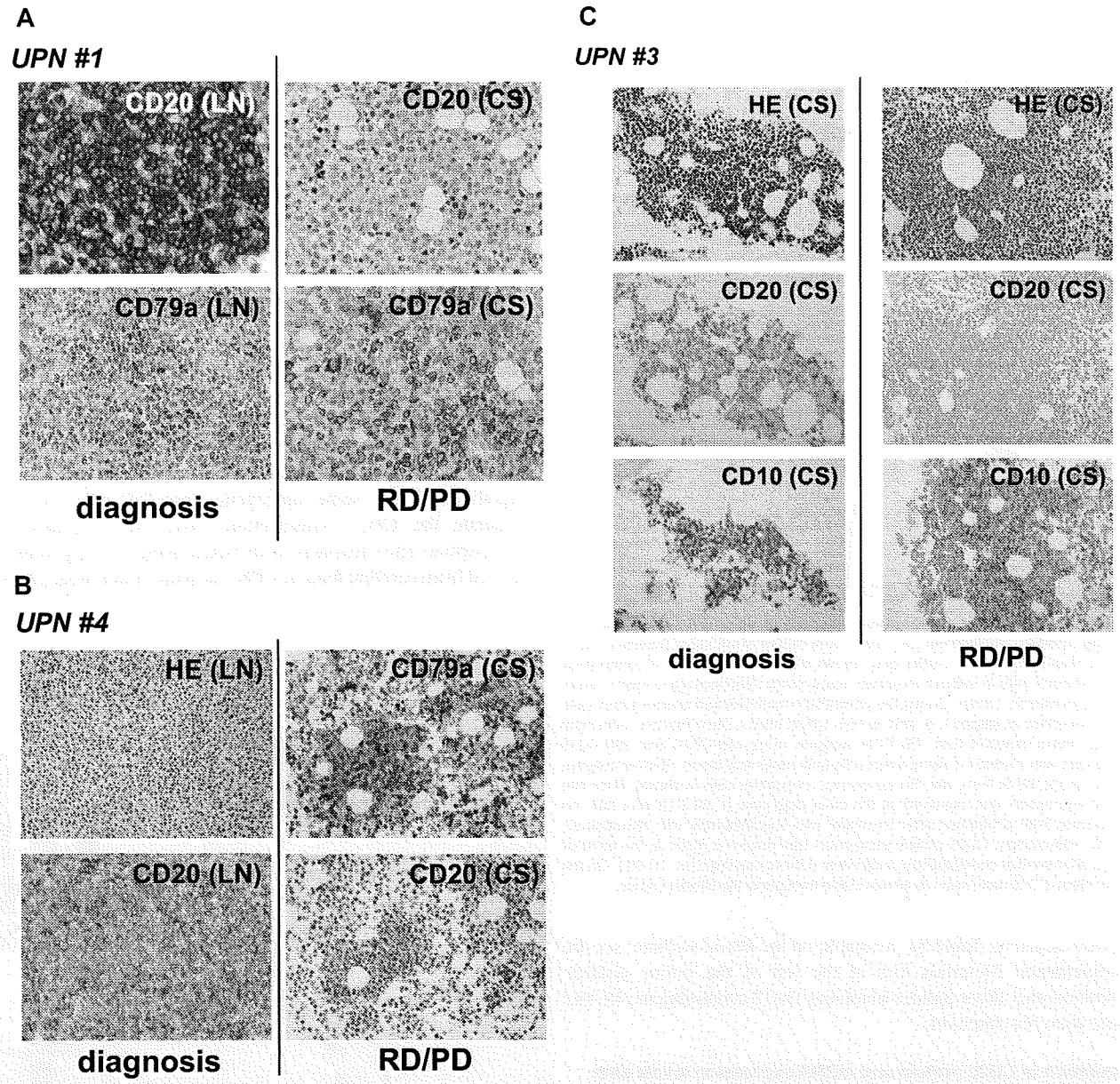

Figure 1. CD20 protein–negative phenotypic changes in CD20-positive B-cell lymphoma patients after treatment with rituximab-containing chemotherapy. Tissue samples (LN, lymph nodes; CS, bone marrow clot section) obtained from UPNs 1 (A), 4 (B), and 3 (C) in Table 2 were analyzed by IHC using anti-CD20, anti-CD79a, and anti-CD10 antibodies. Anti-CD79a antibody was used for detection of B cells. Note that CD20 was positive at the time of initial diagnosis in these patients, and that the CD20-negative phenotypic change was observed during the relapse/progression period. Original magnifications, ×400 (A) and ×200 (B,C) (Olympus BX51TF microscope, Olympus, Tokyo, Japan, and Nikon DS-Fi1 camera, Nikon, Tokyo, Japan). HE indicates hematoxylin and eosin staining; and RD/PD, relapse/progression of disease.

Table 3. Response against salvage chemotherapies for the 36 patients who showed relapse or PD after rituximab-containing chemotherapies.

	CD20 expression		
Response	–	+	N.D.
CR	0	5	3
PR	0	1	3
SD	0	1	1
RD/PD	0	2	2
Death	5	5	8
Total cases	5	14	17

These outcomes were evaluated in July, 2007.

CR indicates complete remisson; PR, partial response; SD, stable disease; RD/PD, relapse/progression; and N.D., Not determined.

Genetic abnormalities in the *CD20* gene

Genomic DNA mutations in the coding sequence (CDS) of the *CD20* gene, also known as the *MS4A1* gene, were also analyzed in the 5 patients. If the mutations were located in specific domains that are recognized by anti-CD20 antibodies including rituximab, those mutations might be related to resistance to rituximab and/or the CD20-negative phenotype. As indicated in Table 2, the change in serine 97 to phenylalanine (S97F; TCC → TTC) in unique patient number (UPN) 1 and valine 247 to isoleucine (V247I; GTT → ATT) in UPN 2 were confirmed in 2 clones each of 16 and 10 clones, respectively. In the other 3 cases, no genetic mutations in the *MS4A1* CDS were detected. Chromosomal analysis by G-banding was also performed using tumor cells obtained from each patient in both the initial diagnosis (CD20-positive) and at the time of RD/PD

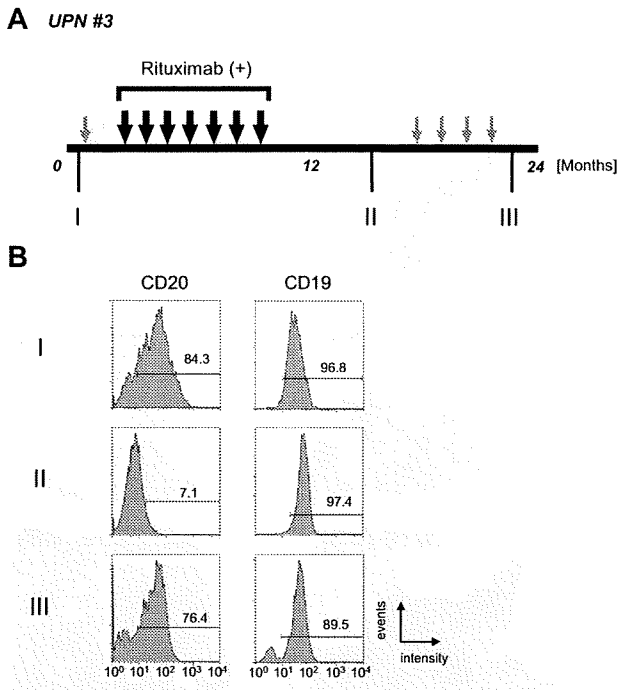

Figure 2. Alteration of CD20 protein expression on B-cell lymphoma cells during disease progression. (A) The clinical course of UPN 3 is depicted briefly. Large black arrows and smaller gray arrows indicate one course of combination chemotherapy with or without rituximab, respectively. Rituximab (375 mg/m^2 each) was administered 7 times. During the patient's 24-month clinical course, tumor cells were harvested at stages I, II, and III from lymph nodes, bone marrow, peripheral blood, and/or cerebral fluid. (B) FCM analysis using anti-CD20 and anti-CD19 antibodies was carried out using tumor cells from peripheral blood. Positive cells are shown in the black lines, and the percentage of positive cells is shown. Note that CD20 expression was observed at the initial diagnosis (I, 84.3%), and that the expression then diminished after treatment with chemotherapy with rituximab (II, 7.1%). Interestingly, CD20 protein expression was observed again at the terminal stage after several chemotherapy treatments without rituximab (III, 76.4%). On the other hand, CD19 expression level was stable throughout the clinical course.

(CD20-negative; Table S1, available on the *Blood* website; see the Supplemental Materials link at the top of the online article). Chromosomal abnormalities involving 11q12 containing the *MS4A1* gene were not observed.

Alteration of CD20 protein and mRNA expression levels after treatment with rituximab

As shown in Figure 1, CD20 protein expression by IHC analysis is altered after chemotherapy with rituximab. The clinical course of UPN 3 is depicted briefly in Figure 2A. FCM analyses using appropriate lymphoma tissues from lymph nodes, peripheral blood, bone marrow, and/or cerebral fluid were performed at admission (I), upon relapse after treatment with rituximab-containing combination chemotherapy (II), and at the end stage of disease after salvage chemotherapy without rituximab (III). The results of FCM analysis using peripheral blood, which contains lymphoma cells, are shown in Figure 2B. Interestingly, CD20 protein expression recognized by FCM analysis was significantly diminished at stage II, but was reversed at stage III. At stage II, CD20-negative lymphoma cell infiltration into the cerebral fluid was also confirmed by FCM analysis (data not shown). On the other hand, CD19 expression, which is also present on B-cell lymphoma cells, was detected constantly throughout the clinical course (Figure 2B right column). Semiquantitative RT-PCR (Figure 3A) and quantitative RT-PCR (Figure 3B) show that the mRNA expression level of *CD20* was significantly altered in each stage. CD20 mRNA expression was faintly observed at stage II (Figure 3B column 4) when CD20 protein expression was barely detectable with FCM (Figure 2B) and IHC (Figure 1C). In UPN 4, CD20 mRNA expression levels were determined by RT-PCR using tumor samples obtained before and after treatment with rituximab-containing chemotherapy (Figure 3C,D). Similar to UPN 3, CD20 mRNA expression was significantly decreased, and no protein expression was detected with IHC (Figure 1B). These findings suggest that CD20 protein expression is mainly regulated at the transcriptional level, and that the expression may be down-regulated in patients who show CD20-negative transformation after treatment with rituximab.

Epigenetic regulation of *CD20* gene expression after treatment with rituximab

These findings suggest that CD20 expression is partly epigenetically regulated by factors such as rituximab treatment surrounding tumor cells, or that CD20-negative tumor cells are able to grow selectively during rituximab treatment. If the CD20-negative B cells still possess the capability to express CD20 protein, we hypothesized that some epigenetic drugs[38,39] may be able to stimulate the *CD20* transcription. First, we examined *CD20* transcription after treatment with 5-Aza using primary tumor cells derived from cerebral fluid of UPN 3 at stage II in Figure 2A, which

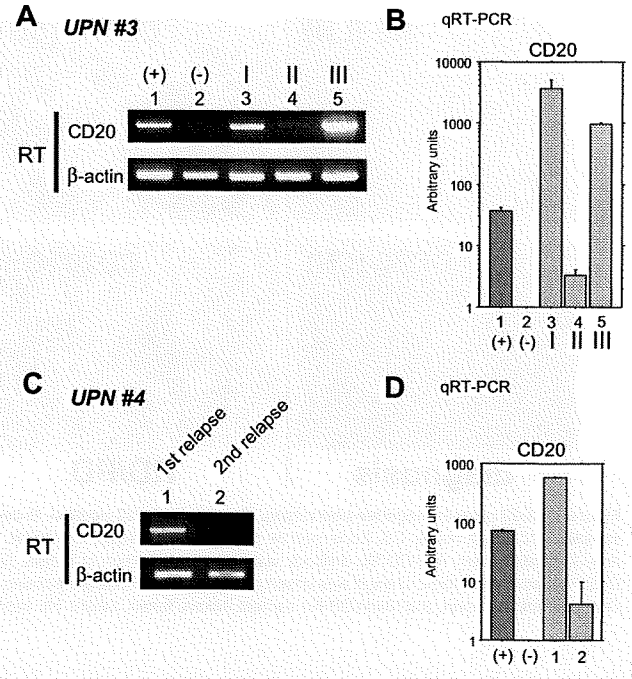

Figure 3. Alteration of CD20 mRNA expression in B-cell lymphoma cells during the clinical course. (A) RT-PCR (RT) was performed using total RNA from the same tumor cells as in Figure 2B (UPN 3 in Table 2). As positive and negative controls, total RNA from Raji and 293T cells was used (lanes 1 and 2), respectively. I, II, and III (lanes 3-5) correspond to the clinical stages depicted in Figure 2A. (B) Quantitative RT-PCR was performed using the same RNA as in panel A. Arbitrary units of CD20 mRNA expression are indicated in the vertical axis. Note that faint expression of CD20 mRNA could be seen at stage II (column 4) despite a loss of CD20 surface protein expression as shown in Figure 2B. (C) CD20 mRNA expression in the lymphoma cells of UPN 4 (Table 2) was also analyzed. Tumor cells were derived from cerebral fluid at the first relapse after chemotherapy without rituximab (lane 1). Although complete remission was obtained after using rituximab-containing salvage chemotherapy, a second relapse occurred. Tumor cells were once again harvested from this patient's cerebral fluid and analyzed (lane 2). (D) Quantitative RT-PCR was also performed using the same RNA as in (C). Note that CD20 mRNA expression was significantly diminished but could still be observed. In these cells, CD20 protein expression was undetectable using FCM or IHC as indicated in Table 2. Positive and negative controls derived from Raji and 293T cells are indicated by + and −, respectively.

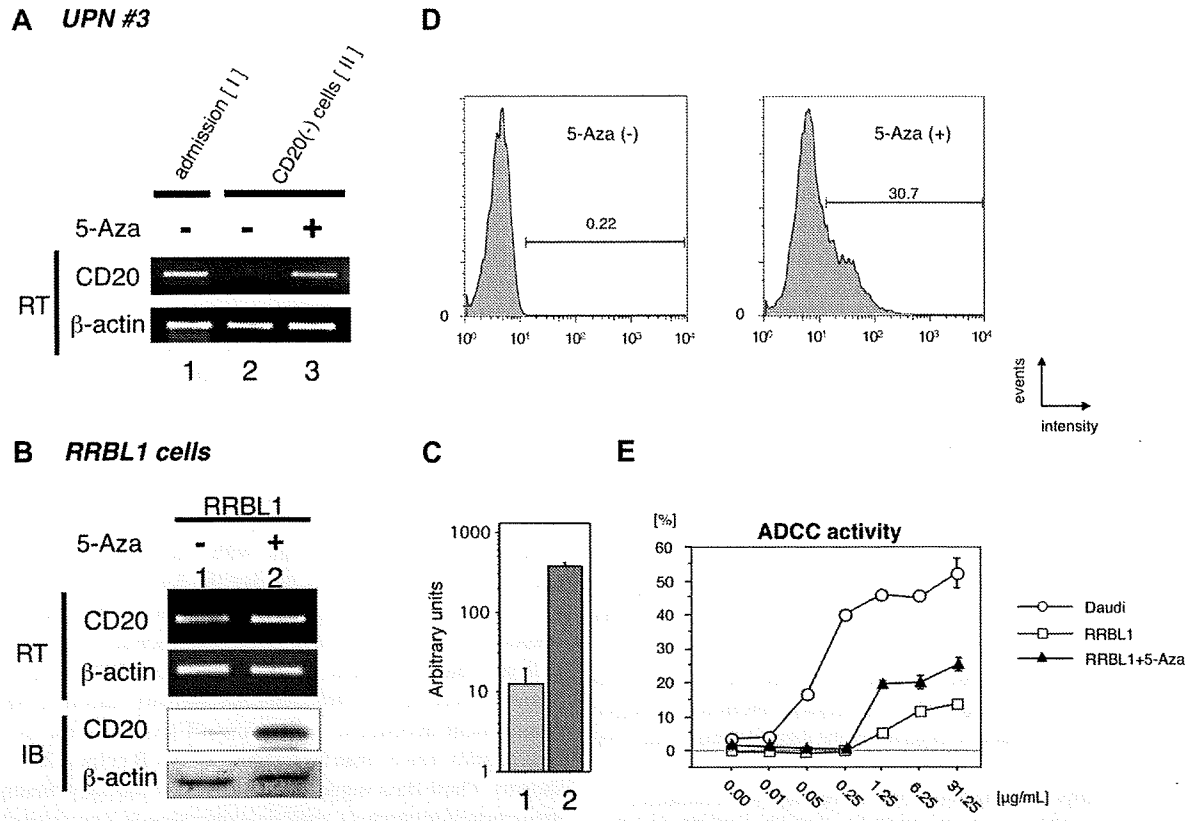

Figure 4. Restoration of CD20 mRNA and protein expression by treatment with the DNA methyltransferase inhibitor 5-Aza. (A) Primary B-cell lymphoma cells, which showed a CD20 protein-negative phenotype from UPN 3, were incubated with or without 5-Aza. Total RNA was prepared, and semiquantitative RT-PCR was performed. Restoration of CD20 mRNA expression after treatment with 5-Aza was observed in lane 3. As a positive control, tumor cells obtained at the initial diagnosis of that same patient were used in lane 1. (B) The CD20 protein-negative B-cell lymphoma cell line RRBL1,[32] which was derived from UPN 5 in Table 2, was incubated in culture medium with or without 5-Aza. After preparation of total RNA and whole-cell lysates from these cells, semiquantitative RT-PCR and immunoblotting (IB) were performed. Up-regulation of CD20 mRNA and protein expression was observed as shown in lane 2. (C) Quantitative RT-PCR was performed using the same mRNA as in (B). We observed an up-regulation of more than 10-fold in CD20 mRNA after treatment with 5-Aza (column 2). (D) RRBL1 cells were treated with 5-Aza under the same conditions as in (B), and FCM analysis using anti-CD20 antibody was performed. After treatment with 5-Aza, 30.7% of RRBL1 cells showed a CD20-positive phenotype. Positive cells are shown with black lines, and the percentage of positive cells is also shown. (E) In vitro ADCC analysis using the ^{51}Cr-release assay. Cells from the CD20-positive B-cell lymphoma/leukemia cell lines Daudi and RRBL1 treated with or without 5-Aza were used for this assay. In Daudi cells (○), but not in RRBL1 cells (□), cytotoxic activity was observed in the presence of rituximab in a dose-dependent manner. Partial restoration of rituximab sensitivity in RRBL1 cells was observed after treatment with 5-Aza (▲). Error bars indicate plus or minus 1 standard deviation.

showed a CD20-negative phenotype. As a CD20-positive control, lymphoma cells at the initial diagnosis from the same patient were used (Figure 4A lane 1). After treatment with 5-Aza in vitro, significant stimulation of CD20 expression was observed (Figure 4 lane 3).

Previously, we established the CD20-negative B-cell lymphoma cell line RRBL1,[32] which was derived from CD20-negative tumor cells in peripheral blood from a patient (UPN 5 in Table 2). Next, we performed the same assay using these cells (Figure 4B), and we were able to show up-regulation of CD20 mRNA expression (Figure 4B,C). CD20 protein expression induction was also confirmed by immunoblotting (Figures 4B, IB). Thus, these data, showing that CD20 expression could be stimulated within a few days, suggested that CD20 expression is down-regulated by epigenetic mechanisms.

Restoration of rituximab sensitivity in CD20-negative cells after treatment with 5-Aza in vitro

From these findings, we hypothesized that rituximab sensitivity would be restored if we could stimulate CD20 protein expression on the surface of CD20-negative transformed lymphoma cells. To test this hypothesis, we performed FCM analysis and an in vitro ADCC assay using RRBL1 cells with or without 5-Aza treatment. As shown in Figure 4D, CD20 protein expression was induced on the surface of 30.7% of RRBL1 cells after treatment with 5-Aza. Using these cells with or without 5-Aza treatment, an in vitro ^{51}Cr-release assay was performed to confirm ADCC activity induced by rituximab (Figure 4E). Daudi cells were used as CD20-positive rituximab-sensitive control cells. In the presence of rituximab, cell death was observed in a dose-dependent manner in Daudi cells. In contrast, the percentage of RRBL1 cells undergoing cell death was significantly lower despite the high concentration of rituximab. RRBL1 cells treated with 5-Aza showed partial rituximab sensitivity compared with RRBL1 cells not treated with 5-Aza. These experiments were done in triplicate and repeated at least 3 times, with similar results. These data suggest that CD20 expression and rituximab sensitivity could be restored in some cases using epigenetic drug treatment even when CD20-negative transformation results from rituximab treatment. Further experiments using patients' primary samples and an in vivo system will be required to further explore this idea.

Discussion

Rituximab is a clinically important antitumor monoclonal antibody targeting the CD20 surface antigen expressed on B-cell malignancies. However, its effectiveness is sometimes unsatisfactory since a significant percentage of patients treated with rituximab-containing

chemotherapy showed relapse or progression.[3,6,40] In this report, we also estimated that RD/PD after treatment with rituximab was observed in almost 30% of B-cell lymphoma patients after treatment with combination chemotherapies with rituximab. Importantly, not all patients who show RD/PD demonstrate resistance to rituximab. In fact, some patients were sensitive to retreatment with rituximab-containing salvage chemotherapies (data not shown). We may need to define "rituximab resistance" more carefully by monitoring each patient's clinical course.

A CD20-negative phenotypic change was observed in 26.3% of patients for whom tumor resampling (rebiopsy) was carried out (Table 1). We generally perform rebiopsies when tumor progression becomes very aggressive or when the manner of tumor expansion significantly changes during clinical observation. If we had carried out resampling on every RD/PD patient, the percentage of patients with CD20-negative transformations may have been much lower. Thus, examination of more patients will be critical. One important observation about the CD20-negative phenotypic change is that all 5 patients died from their disease progression within 1 year after showing a CD20-negative transformation (Tables 2,3). This observation may indicate that a loss of CD20 expression is partly related to poor prognosis. In our study, however, patients' backgrounds varied (eg, age, sex, pathologic findings, chemotherapy regimens, and organ function). A larger patient sample is warranted to determine the significance of the loss of CD20 expression.

It is noteworthy that CD20 mRNA expression was confirmed by RT-PCR even in those tumor cells that showed a CD20 protein-negative phenotype using IHC, FCM, and immunoblotting (Figure 3). In one case (Figure 3, UPN 3), expression of CD20 mRNA and protein were observed again after salvage chemotherapy without rituximab. Clonal evolution may be one reason for the alteration of CD20 mRNA and protein expression patterns in the same patient either with or without rituximab. However, our finding of the restoration of CD20 mRNA and protein expression within 3 days after treatment with 5-Aza (Figure 4) may instead support the idea that expression is regulated by epigenetic mechanisms, rather than by the alteration of several tumor clones.

We cannot exclude the possibility that genetic alteration in tumor cells that affects the expression of transcription factors PU.1, Pip, and Oct2, which are thought to be critical for *MS4A1* (*CD20*) gene expression,[41] may contribute to the aberrant *CD20* transcriptional regulation. We analyzed the methylation status of cytosine guanine dinucleotides (CpGs) in *CD20* promoters almost 1000 bp upstream from the transcription start site to determine the mechanism of transcription up-regulation by 5-Aza treatment. Interestingly, CpG islands do not exist in the promoter site, and only 4 CG sequences can be observed in that region. Methylation of the 4 CG sites was not observed in the tumor cells from UPN 5 and RRBL1 cells using bisulfite sequencing (data not shown). Mechanisms other than DNA methylation of the *CD20* promoter may also be responsible for aberrant transcription down-regulation.

It is also possible that down-regulation of CD20 protein via such mechanisms as microRNA, protein folding, exportation, or glycosylation may occur. A recent report suggested the possibility that both *CD20* gene expression (at the pre- and posttranscriptional level) and protein down-regulation are related to the loss of CD20 protein expression after treatment with rituximab in vitro, resulting in rituximab resistance.[10] In addition, down-regulation of CD20 protein surface expression by internalization into the cytoplasm was also observed in some specific cases.[16,42] Further molecular analysis of the down-regulation of CD20 protein after treatment with rituximab is needed.

Another interesting finding in our study is that all of the patients showed a CD20-negative phenotypic change were diagnosed as DLBCL. Two cases were diagnosed as FL at their first admission, but both were transformed into DLBCL when a CD20-negative change was observed. Furthermore, a CD20-negative change was confirmed in all 5 cases using tumor cells derived from the bone marrow and/or cerebral fluid. These findings may suggest that the clinical entity and progression pattern is partly related to CD20-negative phenotypic transformation. Further studies will be needed to confirm this idea.

Genetic mutations in the *CD20* coding sequence were also observed in 2 cases, as shown in Table 2. These mutations led to amino acid alterations, including S97F and V247I, which are located at the second transmembrane domain and the C-terminal intracellular domain, respectively. A recent report suggested that neither site is recognized directly by rituximab.[43] Although it is possible that these alterations led to a conformational change in the CD20 protein that interferes with rituximab binding, a more attractive explanation may be that the loss of expression is much more critical for resistance to rituximab than we originally suspected. Preliminary data using fluorescence-labeled rituximab indicate that rituximab fails to bind to RRBL1 cells (CD20-negative B cells) in vitro (data not shown), and that ADCC and complement-dependent cytotoxicity (CDC) activity in vitro are significantly lower than in CD20-positive B cells (CDC; data not shown). These data suggest that the loss of antibody binding due to the down-regulation of antigen expression is one critical mechanism underlying rituximab resistance. Further investigation will be needed to expand these observations.

Our observations also revealed a population of cells that are rituximab-resistant despite the presence of CD20 protein expression as observed by FCM, IHC, and immunoblotting (data not shown). In those patients, molecular mechanisms other than a loss of protein expression may have occurred, such as an amino acid alteration resulting from a genetic mutation of the *MS4A1* gene, a posttranslational modification of the CD20 protein, abnormalities in the CD20 signal transduction pathway, antiapoptotic mechanisms of tumor cells, or aberrant metabolism of rituximab.[9,44,45] The detailed mechanisms of these and other possibilities are still unclear.

Finally, in the specific cases reported herein, 5-Aza can stimulate CD20 mRNA and protein expression, resulting in the restoration of rituximab sensitivity in vitro. The DNA methyltransferase inhibitors 5-azacytidine and 5-Aza have been used in patients suffering from hematologic malignancies such as myelodysplastic syndrome.[38,39,46] In the future, a combination of molecular targeting therapy using 5-Aza and rituximab may prove to be a unique strategy as a salvage therapy for CD20-negative transformed B-cell malignancies in certain patients. Further analysis of patients' primary cells and in vivo analysis using mouse xenograft lymphoma models are required.

Acknowledgments

We thank Tomoka Wakamatsu, Yukie Konishi, Mari Otsuka, Eriko Ushida, and Chieko Kataoka for valuable laboratory assistance. We also thank Yoko Kajiura, Yasuhiko Miyata, and Yuka Nomura for the FCM data analysis.

This work was supported in part by a Grant-in-Aid for Cancer Research (19-8) from the Ministry of Health, Labor and Welfare, a Grant-in-Aid from the National Institute of Biomedical Innovation, and

a Grant-in-Aid for Scientific Research (20591116) from the Ministry of Education, Culture, Sports, Science and Technology, Japan.

Authorship

J.H. and A.T. designed experiments, performed research, analyzed data, and wrote the paper; T.S. and K.S. prepared clinical samples and performed research; M.I. and S.N. performed pathologic analyses; H.K. and T.K. analyzed data, designed experiments, and interpreted data; and T.N. supervised experiments and wrote the paper.

Conflict-of-interest disclosure: H.K. is a consultant for a Kyowa Hakko Kogyo (Tokyo, Japan), and T.K. is funded by Chugai Pharmaceutical (Tokyo, Japan) and for Zenyaku Kogyo (Tokyo, Japan). The other authors declare no competing financial interests.

Correspondence: Akihiro Tomita, Department of Hematology and Oncology, Nagoya University Graduate School of Medicine, Tsurumai-cho 65, Showa-ku, Nagoya 466-8550, Japan; e-mail; atomita@med.nagoya-u.ac.jp.

References

1. Cheson BD. Monoclonal antibody therapy for B-cell malignancies. Semin Oncol. 2006;33:S2-14.
2. Imai K, Takaoka A. Comparing antibody and small-molecule therapies for cancer. Nat Rev Cancer. 2006;6:714-727.
3. Coiffier B, Lepage E, Briere J, et al. CHOP chemotherapy plus rituximab compared with CHOP alone in elderly patients with diffuse large-B-cell lymphoma. N Engl J Med. 2002;346:235-242.
4. Herold M, Haas A, Srock S, et al. Rituximab added to first-line mitoxantrone, chlorambucil, and prednisolone chemotherapy followed by interferon maintenance prolongs survival in patients with advanced follicular lymphoma: an East German Study Group Hematology and Oncology Study. J Clin Oncol. 2007;25:1986-1992.
5. Forstpointner R, Unterhalt M, Dreyling M, et al. Maintenance therapy with rituximab leads to a significant prolongation of response duration after salvage therapy with a combination of rituximab, fludarabine, cyclophosphamide, and mitoxantrone (R-FCM) in patients with recurring and refractory follicular and mantle cell lymphomas: results of a prospective randomized study of the German Low Grade Lymphoma Study Group (GLSG). Blood. 2006;108:4003-4008.
6. Habermann TM, Weller EA, Morrison VA, et al. Rituximab-CHOP versus CHOP alone or with maintenance rituximab in older patients with diffuse large B-cell lymphoma. J Clin Oncol. 2006;24:3121-3127.
7. Pfreundschuh M, Trumper L, Osterborg A, et al. CHOP-like chemotherapy plus rituximab versus CHOP-like chemotherapy alone in young patients with good-prognosis diffuse large-B-cell lymphoma: a randomised controlled trial by the MabThera International Trial (MInT) Group. Lancet Oncol. 2006;7:379-391.
8. Igarashi T, Kobayashi Y, Ogura M, et al. Factors affecting toxicity, response and progression-free survival in relapsed patients with indolent B-cell lymphoma and mantle cell lymphoma treated with rituximab: a Japanese phase II study. Ann Oncol. 2002;13:928-943.
9. Smith MR. Rituximab (monoclonal anti-CD20 antibody): mechanisms of action and resistance. Oncogene. 2003;22:7359-7368.
10. Czuczman MS, Olejniczak S, Gowda A, et al. Acquirement of rituximab resistance in lymphoma cell lines is associated with both global CD20 gene and protein down-regulation regulated at the pretranscriptional and posttranscriptional levels. Clin Cancer Res. 2008;14:1561-1570.
11. Olejniczak SH, Hernandez-Ilizaliturri FJ, Clements JL, Czuczman MS. Acquired resistance to rituximab is associated with chemotherapy resistance resulting from decreased Bax and Bak expression. Clin Cancer Res. 2008;14:1550-1560.
12. Macor P, Tripodo C, Zorzet S, et al. In vivo targeting of human neutralizing antibodies against CD55 and CD59 to lymphoma cells increases the antitumor activity of rituximab. Cancer Res. 2007; 67:10556-10563.
13. Cruz RI, Hernandez-Ilizaliturri FJ, Olejniczak S, et al. CD52 over-expression affects rituximab-associated complement-mediated cytotoxicity but not antibody-dependent cellular cytotoxicity: preclinical evidence that targeting CD52 with alemtuzumab may reverse acquired resistance to rituximab in non-Hodgkin lymphoma. Leuk Lymphoma. 2007;48:2424-2436.
14. Terui Y, Sakurai T, Mishima Y, et al. Blockade of bulky lymphoma-associated CD55 expression by RNA interference overcomes resistance to complement-dependent cytotoxicity with rituximab. Cancer Sci. 2006;97:72-79.
15. Takei K, Yamazaki T, Sawada U, Ishizuka H, Aizawa S. Analysis of changes in CD20, CD55, and CD59 expression on established rituximab-resistant B-lymphoma cell lines. Leuk Res. 2006; 30:625-631.
16. Jilani I, O'Brien S, Manshuri T, et al. Transient down-modulation of CD20 by rituximab in patients with chronic lymphocytic leukemia. Blood. 2003;102:3514-3520.
17. Bannerji R, Kitada S, Flinn IW, et al. Apoptotic-regulatory and complement-protecting protein expression in chronic lymphocytic leukemia: relationship to in vivo rituximab resistance. J Clin Oncol. 2003;21:1466-1471.
18. Treon SP, Mitsiades C, Mitsiades N, et al. Tumor cell expression of CD59 is associated with resistance to CD20 serotherapy in patients with B-cell malignancies. J Immunother. 2001;24:263-271.
19. Golay J, Lazzari M, Facchinetti V, et al. CD20 levels determine the in vitro susceptibility to rituximab and complement of B-cell chronic lymphocytic leukemia: further regulation by CD55 and CD59. Blood. 2001;98:3383-3389.
20. Kinoshita T, Nagai H, Murate T, Saito H. CD20-negative relapse in B-cell lymphoma after treatment with rituximab. J Clin Oncol. 1998;16:3916.
21. Schmitz K, Brugger W, Weiss B, Kaiserling E, Kanz L. Clonal selection of CD20-negative non-Hodgkin's lymphoma cells after treatment with anti-CD20 antibody rituximab. Br J Haematol. 1999;106:571-572.
22. Davis TA, Czerwinski DK, Levy R. Therapy of B-cell lymphoma with anti-CD20 antibodies can result in the loss of CD20 antigen expression. Clin Cancer Res. 1999;5:611-615.
23. Chu PG, Chen YY, Molina A, Arber DA, Weiss LM. Recurrent B-cell neoplasms after rituximab therapy: an immunophenotypic and genotypic study. Leuk Lymphoma. 2002;43:2335-2341.
24. Massengale WT, McBurney E, Gurtler J. CD20-negative relapse of cutaneous B-cell lymphoma after anti-CD20 monoclonal antibody therapy. J Am Acad Dermatol. 2002;46:441-443.
25. Kennedy GA, Tey SK, Cobcroft R, et al. Incidence and nature of CD20-negative relapses following rituximab therapy in aggressive B-cell non-Hodgkin's lymphoma: a retrospective review. Br J Haematol. 2002;119:412-416.
26. Alvaro-Naranjo T, Jaen-Martinez J, Guma-Padro J, Bosch-Princep R, Salvado-Usach MT. CD20-negative DLBCL transformation after rituximab treatment in follicular lymphoma: a new case report and review of the literature. Ann Hematol. 2003;82:585-588.
27. Clarke LE, Bayerl MG, Ehmann WC, Helm KF. Cutaneous B-cell lymphoma with loss of CD20 immunoreactivity after rituximab therapy. J Cutan Pathol. 2003;30:459-462.
28. Haidar JH, Shamseddine A, Salem Z, et al. Loss of CD20 expression in relapsed lymphomas after rituximab therapy. Eur J Haematol. 2003;70:330-332.
29. Rawal YB, Nuovo GJ, Frambach GE, Porcu P, Baiocchi RA, Magro CM. The absence of CD20 messenger RNA in recurrent cutaneous B-cell lymphoma following rituximab therapy. J Cutan Pathol. 2005;32:616-621.
30. Goteri G, Olivieri A, Ranaldi R, et al. Bone marrow histopathological and molecular changes of small B-cell lymphomas after rituximab therapy: comparison with clinical response and patients outcome. Int J Immunopathol Pharmacol. 2006; 19:421-431.
31. Ferreri AJ, Dognini GP, Verona C, Patriarca C, Doglioni C, Ponzoni M. Re-occurrence of the CD20 molecule expression subsequent to CD20-negative relapse in diffuse large B-cell lymphoma. Haematologica. 2007;92:e1-2.
32. Tomita A, Hiraga J, Kiyoi H, et al. Epigenetic regulation of CD20 protein expression in a novel B-cell lymphoma cell line, RRBL1, established from a patient treated repeatedly with rituximab-containing chemotherapy. Int J Hematol. 2007;86: 49-57.
33. Harris NL, Jaffe ES, Diebold J, et al. World Health Organization classification of neoplastic diseases of the hematopoietic and lymphoid tissues: report of the Clinical Advisory Committee meeting-Airlie House, Virginia, November 1997. J Clin Oncol. 1999;17:3835-3849.
34. Cheson BD, Horning SJ, Coiffier B, et al. Report of an international workshop to standardize response criteria for non-Hodgkin's lymphomas: NCI Sponsored International Working Group. J Clin Oncol. 1999;17:1244.
35. Ninomiya M, Abe A, Yokozawa T, et al. Establishment of a myeloid leukemia cell line, TRL-01, with MLL-ENL fusion gene. Cancer Genet Cytogenet. 2006;169:1-11.
36. Atsumi A, Tomita A, Kiyoi H, Naoe T. Histone deacetylase 3 (HDAC3) is recruited to target promoters by PML-RARalpha as a component of the N-CoR co-repressor complex to repress transcription in vivo. Biochem Biophys Res Commun. 2006;345:1471-1480.
37. Tomita A, Buchholz DR, Obata K, Shi YB. Fusion protein of retinoic acid receptor alpha with promyelocytic leukemia protein or promyelocytic leukemia zinc finger protein recruits N-CoR-TBLR1 corepressor complex to repress transcription in vivo. J Biol Chem. 2003;278: 30788-30795.
38. Egger G, Liang G, Aparicio A, Jones PA. Epigenetics in human disease and prospects for epigenetic therapy. Nature. 2004;429:457-463.
39. Yoo CB, Jones PA. Epigenetic therapy of cancer: past, present and future. Nat Rev Drug Discov. 2006;5:37-50.

40. van Oers MH, Klasa R, Marcus RE, et al. Rituximab maintenance improves clinical outcome of relapsed/resistant follicular non-Hodgkin's lymphoma, both in patients with and without rituximab during induction: results of a prospective randomized phase III intergroup trial. Blood. 2006;108;3295-3301.
41. Himmelmann A, Riva A, Wilson GL, Lucas BP, Thevenin C, Kehrl JH. PU.1/Pip and basic helix loop helix zipper transcription factors interact with binding sites in the CD20 promoter to help confer lineage- and stage-specific expression of CD20 in B lymphocytes. Blood. 1997;90: 3984-3995.
42. Lapalombella R, Yu B, Triantafillou G, et al. Lenalidomide down-regulates the CD20 antigen and antagonizes direct and antibody-dependent cellular cytotoxicity of rituximab on primary chronic lymphocytic leukemia cells. Blood. 2008;113: 5180-5185.
43. Binder M, Otto F, Mertelsmann R, Veelken H, Trepel M. The epitope recognized by rituximab. Blood. 2006;108:1975-1978.
44. Bonavida B. Rituximab-induced inhibition of antiapoptotic cell survival pathways: implications in chemo/immunoresistance, rituximab unresponsiveness, prognostic and novel therapeutic interventions. Oncogene. 2007;26:3629-3636.
45. Glennie MJ, French RR, Cragg MS, Taylor RP. Mechanisms of killing by anti-CD20 monoclonal antibodies. Mol Immunol. 2007;44:3823-3837.
46. Laird PW. Cancer epigenetics. Hum Mol Genet. 2005;14:R65-R76.

Image 4

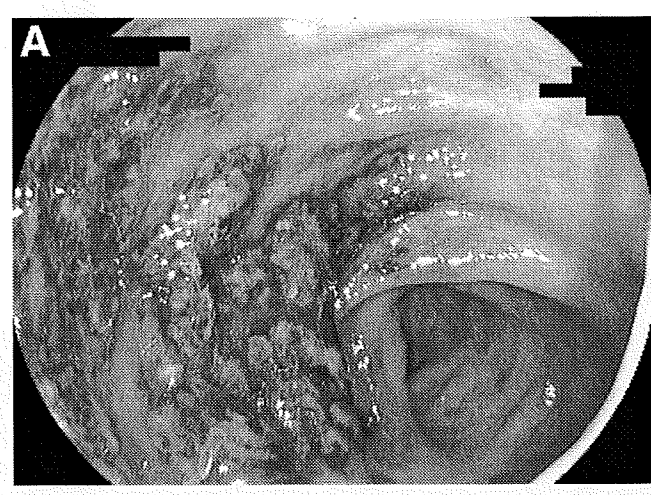

See related article, Miyazaki M et al on page e32 in *CGH*.

Question: A 34-year-old man with multiple myeloma underwent reduced-intensity cord blood stem cell transplantation (RI-CBSCT) 20 months after the initial diagnosis, followed by prophylactic administration of tacrolimus, a calcineurin inhibitor, for preventing graft-versus-host disease (GVHD). On day 55, the patient complained of watery diarrhea. Neither *Clostridium difficile* toxin nor enteric pathogens were detected in the stool. Laboratory data at onset of symptoms were as follows: platelet count decreased from $210 \times 10^9/mm^3$ to $90 \times 10^9/mm^3$ within 2 days; hemoglobin was 8.7 g/dL. Myeloma cells were seen in peripheral blood. Serum indirect bilirubin was 1.6 mg/dL (normal, 0.2–1.1 mg/dL) and the lactate dehydrogenase level was 267 IU/L (normal, 129–241 IU/L); serum haptoglobin was undetectable. C-reactive protein level was 2.3 mg/dL (normal, 0–0.2 mg/dL). Blood tacrolimus trough level was 8.9 ng/mL (adjusted trough level for GVHD, around 10 ng/mL). Colonoscopy performed on day 59 revealed segmental longitudinal ulcerations with hemorrhagic edematous mucosa in the transverse colon (Figure *A*).

What is your diagnosis of this patient?

Look on page 2418 for the answer and see the GASTROENTEROLOGY web site (www.gastrojournal.org) for more information on submitting your favorite image to Clinical Challenges and Images in GI.

SHUJI YAMAMOTO, MD
HIROSHI NAKASE, MD, PhD
TSUTOMU CHIBA, MD, PhD
Department of Gastroenterology and Hepatology
Graduate School of Medicine
Kyoto University
Kyoto, Japan
KOUHEI YAMASHITA, MD, PhD
Department of Hematology and Oncology
Graduate School of Medicine
Kyoto University
Kyoto, Japan
MASAFUMI ITO, MD, PhD
Department of Pathology
Japanese Red Cross
Nagoya First Hospital
Nagoya, Japan

Conflicts of interest
The authors disclose no conflicts.

0016-5085/59645/$36.00
doi:10.1053/j.gastro.2009.02.086

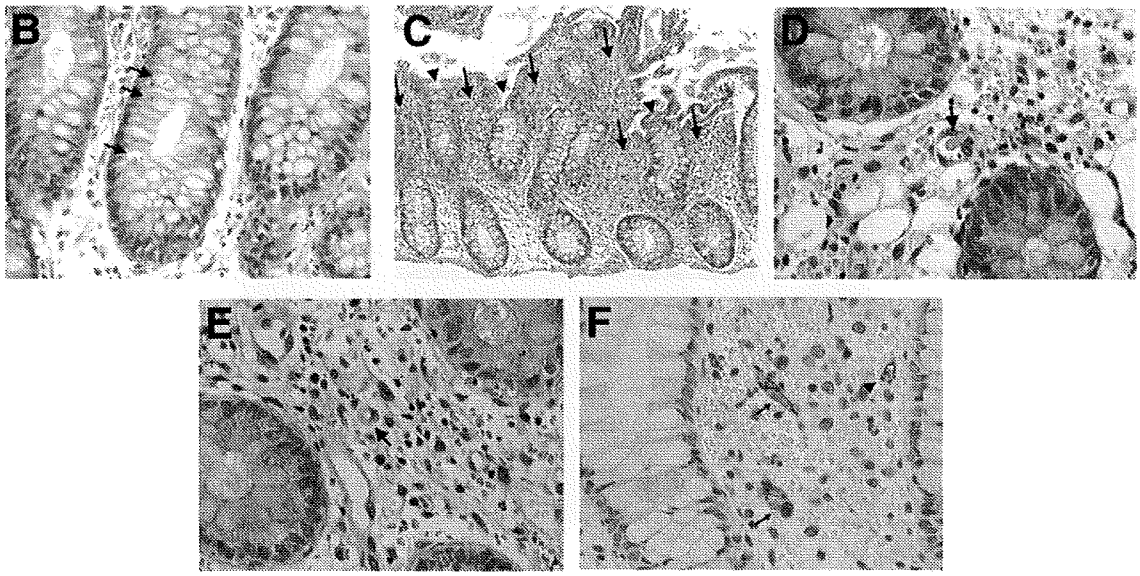

Answer to the Clinical Challenges and Images in GI Question: Image 4 (page 2067): Transplant-Associated Thrombotic Microangiopathy of the Colon Accompanied by Graft-Versus-Host Disease

Histologic analysis of the biopsy specimen from the edge of the ulcer in the transverse colon revealed crypt epithelial cell apoptosis (Figure *B*, *arrows*). In addition, histologic findings, which are characteristic of transplant-associated thrombotic microangiopathy (TA-TMA), including crypt depletion (Fig *C*, *arrowheads*) and mucosal hemorrhage (Figure *C*, *arrows*), capillary thrombosis (Figure *D*, *arrow*), and hyaline subintimal thickening of vessel walls with red cell fragmentation (Figure *E*, *arrow*) were observed in the same section. Immunohistologic study with anti-CD34 (Figure *F*) showed swelling (*arrows*) and degeneration (*arrowhead*) of endothelial cells in the capillary. The final diagnosis was TA-TMA of the colon accompanied by GI-GVHD. Methylprednisolone for GI-GVHD was administrated and tacrolimus was discontinued to avoid development of TA-TMA. Diarrhea subsided after starting these treatments. Unfortunately, the patient died of relapsed myeloma on day 118 after RI-CBSCT.

TA-TMA is a potentially life-threatening complication of hematopoietic stem cell transplantation,[1] and endothelial injury is likely to be the primary pathogenic event.[2] The clinical presentation of TA-TMA is heterogeneous, which ranges from asymptomatic to fulminant disease, including renal dysfunction and neurologic abnormalities[1]; the gastrointestinal tract is also involved in this disorder.[3] It is important to diagnose accurately whether or not intestinal TA-TMA exists, especially in cases accompanied with GI-GVHD, because calcineurin inhibitors, including tacrolimus and cyclosporine, should be withdrawn after a diagnosis of TMA.[1] There is no report on the characteristic endoscopic findings, however, that distinguish intestinal TA-TMA from GI-GVHD. Interestingly, endoscopic findings in the transverse colon of the present case showed longitudinal ulcerations and hemorrhagic edematous mucosa, which mimicked ischemic colitis, and histology revealed intestinal TA-TMA. Thus, it may be noted that endoscopic findings like ischemic colitis in patients with abdominal symptoms after hematopoietic stem cell transplantation might suggest intestinal TA-TMA.

References

1. Ho VT, Cutler C, Carter S, et al. Blood and marrow transplant clinical trials network toxicity committee consensus summary: thrombotic microangiopathy after hematopoietic stem cell transplantation. Biol Blood Marrow Transplant 2005;11:571–575.
2. Holler E, Kolb HJ, Hiller E, et al. Microangiopathy in patients on cyclosporine prophylaxis who developed acute graft-versus-host disease after HLA-identical bone marrow transplantation. Blood 1989;73:2018–2024.
3. Nishida T, Hamaguchi M, Hirabayashi N, et al. Intestinal thrombotic microangiopathy after allogeneic bone marrow transplantation: a clinical imitator of acute enteric graft-versus-host disease. Bone Marrow Transplant 2004;33:1143–1150.

Brief report

Impact of macrophage infiltration of skin lesions on survival after allogeneic stem cell transplantation: a clue to refractory graft-versus-host disease

Satoshi Nishiwaki,[1] Seitaro Terakura,[1] Masafumi Ito,[2] Tatsunori Goto,[1] Aika Seto,[1] Keisuke Watanabe,[1] Mayumi Yanagisawa,[1] Nobuhiko Imahashi,[1] Shokichi Tsukamoto,[1] Makoto Shimba,[1] Yukiyasu Ozawa,[1] and Koichi Miyamura[1]

Departments of [1]Hematology and [2]Pathology, Japanese Red Cross Nagoya First Hospital, Nagoya, Japan

We retrospectively reviewed 104 biopsy specimens of previously untreated skin acute graft-versus-host disease (GVHD) within 100 days after allogeneic stem cell transplantation, and analyzed the relationship between types of infiltrating cells and clinical outcomes. Counting the total number of CD8$^+$ T cells, CD163$^+$ macrophages, and CD1a$^+$ dendritic cells in 4 fields under original magnification ×200, the infiltration of more than 200 cells of CD163$^+$ macrophages (many macrophages [MM]) was the only significant predictor for refractory GHVD (odds ratio, 3.79; 95% confidence interval, 1.22-11.8; $P = .02$). In 46 patients given steroid treatments, MM was the only significant predictor for refractory acute GVHD (odds ratio, 5.05; 95% confidence interval, 1.19-21.3; $P = .03$). Overall survival of patients with MM was significantly lower than that of those with an infiltration of less than 200 cells of CD163$^+$ macrophages. Macrophage infiltration of skin lesions could be a significant predictive factor for refractory GVHD and a poor prognosis. (Blood. 2009;114: 3113-3116)

Introduction

Macrophages are phagocytic cells with various abilities, such as phagocytosis, antigen-presenting, and secretion of cytokines.[1,2] Recently, it was revealed in human sequential biopsy data that recipient macrophages contributed to acute graft-versus-host disease (GVHD) by antigen-presenting and secreting cytokines, causing the activation and proliferation of CD8$^+$ T cells.[3] We focused on macrophage involvement in acute GVHD, especially on the relationship between the macrophage infiltration of skin lesions and refractory GVHD.

Methods

Between January 1997 and October 2007 at the Japanese Red Cross Nagoya First Hospital, we used skin biopsy specimens within 100 days after allogeneic stem cell transplantation (allo-SCT) of skin lesions clinically considered acute GVHD without any GVHD treatment from 104 patients who underwent allo-SCTs. We analyzed the relationship between types of infiltrating cells and clinical outcomes by counting the total number of CD8$^+$ T cells, CD163$^+$ macrophages, and CD1a$^+$ dendritic cells in 4 fields of a skin biopsy specimen under original magnification ×200. Immunohistochemical analysis using paraffin sections was performed using monoclonal antibodies against CD8, CD163, and CD1a (Novocastra). CD163 is a member of the scavenger receptor cystein-rich superfamily and is an exclusive marker for macrophages, playing a major role in the scavenging components of damaged cells.[4-7]

The endpoints of this study were the outcomes of acute GVHD and overall survival (OS). Acute GVHD was diagnosed and graded according to the consensus criteria.[8] We defined refractory GVHD as that exhibited by patients who had persistent lesions after primary steroid treatments. To establish parameters, we analyzed the numbers of infiltrating CD8$^+$ T cells ($\leq$ 100/4 fields [few T cells; FT] vs $>$ 100/4 fields [many T cells; MT]), numbers of infiltrating CD163$^+$ macrophages ($\leq$ 200/4 fields [few macrophages; FM] vs $>$ 200/4 fields [many macrophages; MM]), disease risk (low vs high), human leukocyte antigen (HLA) disparity (match vs mismatch), donor source (related vs unrelated), graft source (bone marrow vs peripheral blood), age at allo-SCT ($\leq$ 50 years vs $>$ 50 years), conditioning regimen (conventional regimens vs reduced intensity regimens), and skin GVHD stage at biopsy (stages 1-2 vs stages 3-4). A significance level of $P < .05$ was used for all analyses, which were based on all data available as of August 31, 2008. Protocols were approved by the Japanese Red Cross Nagoya First Hospital's Institutional Review Board, and all patients provided informed consent in accordance with the Declaration of Helsinki.

Results and discussion

Table 1 summarizes the characteristics of patients and information gathered about GVHD. We divided patients into 4 groups according to the amount of infiltrating cells (FM and FT, 60.6%; MT and FM, 18.2%; MT and MM, 10.6%; and FT and MM, 10.6%). We noted a striking difference among patients in the types of infiltrating cells in skin GVHD lesions (Figure 1A). The distributions of numbers of infiltrating cells also exhibited a

Submitted March 9, 2009; accepted June 28, 2009. Prepublished online as *Blood* First Edition paper, July 30, 2009; DOI 10.1182/blood-2009-03-209635.

The publication costs of this article were defrayed in part by page charge payment. Therefore, and solely to indicate this fact, this article is hereby marked "advertisement" in accordance with 18 USC section 1734.

Table 1. Information on patient characteristics, acute GVHD, and skin biopsy

Characteristic	Value
Patient characteristics	
Total no. of patients	104
Median age at allo-SCT, y (range)	40.5 (19-61)
Male/female	65/39
Disease risk, low/high	51/53
HLA, match/mismatch	72/32
Donor, unrelated/related	67/37
Graft, BM/PB/CB	89/11/4
Conditioning, conventional/RIST	78/26
Median observation period, mo (range)	13.7 (0.7-120.7)
Acute GVHD	
Stage skin (at the time of biopsy), 1/2/3/4	22/57/25/0
Skin (the maximal severity), 1/2/3/4	16/25/52/11
Gut, 0/1/2/3/4	69/9/8/15/3
Liver, 0/1/2/3/4	82/5/3/9/5
Grade (at the time of the biopsy), I/II/III/IV	58/41/4/1
Grade (the maximal severity), I/II/III/IV	28/44/19/13
Primary steroid treatment, yes/no	46/58
Second treatment, yes/no	18/30
Outcome of GVHD, improved/refractory	84/20
Skin lesion	
Median date of appearance, days (range)	24 (5-81)
Median date of skin biopsy, days (range)	31.5 (6-82)
Median date of highest stage of skin GVHD, days (range)	34 (9-90)
No. of infiltrating $CD8^+$ cells	65 (2-305)
No. of infiltrating $CD163^+$ cells	132.5 (38-372)
No. of infiltrating $CD1a^+$ cells	7 (0-122)

Disease risk low indicates acute leukemia in first remission; CML, in first chronic phase; MDS, refractory anemia or nonmalignant hematologic disease; disease risk high, all other diagnoses; HLA match, identical HLA-A, -B, and -DRB1 loci; HLA mismatch, at least one disparity at one of these loci; BM, bone marrow; PB, peripheral blood; CB, cord blood; and RIST, reduced intensity conditioning regimens.

considerably wide variety (Figure 1B). The median number of infiltrating $CD8^+$ T cells was 65 (range, 2-305), that of infiltrating $CD163^+$ macrophages was 132.5 (range, 38-372), and thatof infiltrating $CD1a^+$ dendritic cells was 7 (range, 0-122). We used 3 skin biopsy specimens of drug rash from autologous transplantation patients as non-GVHD controls; the median numbers of $CD8^+$, $CD163^+$, and $CD1a^+$ infiltrating cells were 11 (range, 6-15), 26 (range, 19-30), and 68 (range, 65-83), respectively. MT was correlated with an HLA mismatch ($P = .047$), grade III-IV acute GVHD ($P = .03$), and MM ($P = .01$), whereas MM was correlated with unrelated donor ($P = .04$), an HLA mismatch ($P = .049$), refractory GVHD ($P = .004$), and MT ($P = .01$) using χ^2 analyses. The sensitivity and specificity of MT for refractory GVHD were 25.0% and 70.5% in all 104 patients, and 25.0% and 73.3% in 46 receiving steroids, whereas those of MM were 43.8% and 82.9%, and 43.8% and 86.7%, respectively.

In 46 patients undergoing steroid treatments, the median date of the appearance of skin lesions was 17.0 days (range, 5-54 days), whereas that of skin biopsy was 27.5 days (range, 6-63 days) and that of the highest skin stage was 32.0 days (range, 9-68 days). Treatments for GVHD were considered for GVHD patients without spontaneous regression and with progression to a higher grade, except for those in which enhanced immunosuppression would not be preferable, such as encephalopathy resulting from calcineurin inhibitor or a pathologic diagnosis of intestinal transplantation-associated microangiopathy.[9,10] The median interval from the initial clinical manifestation of GVHD to the primary treatments was 4.5 days (range, 0-97 days). The dose of prednisolone was 0.5 mg/kg in 4 patients, 1 mg/kg in 20 patients, 2 mg/kg in 19 patients, 500 mg/body in 1 patient, and 1000 mg/body in 2 patients. Only MM was identified as a negative predictive factor for refractory GVHD (Table 2). In 46 patients undergoing steroid treatments, only MM was identified as a negative predictive factor for refractory GVHD (odds ratio, 5.05; 95% confidence interval [CI], 1.19-21.3; $P = .03$).

In the Cox proportional hazard model, age more than 50 years, high risk, and MM were identified as significant risk factors by univariate analyses, with MM and high risk remaining a significant risk in a multivariate analysis (Table 3). OS rates were significantly higher in FM patients compared with those in MM (Figure 1C). Uncontrolled GVHD was the cause of 6 MM patients of 11 (54.5%) who died because of transplantation-related mortality (TRM), whereas in FM patients, 3 of 24 (12.5%) died because of uncontrolled GVHD. The causes of death for the 5 MM patients who did not die of uncontrolled GVHD were infection in 3 patients, intestinal transplantation-associated microangiopathy in 1 patient, and liver failure in 1 patient. In 46 patients who underwent steroid treatments, only MM was identified as a significant risk factor in the Cox proportional hazards model (Hazard ratio 3.25; 95% CI, 1.46-7.26; $P = .004$). OS rates were significantly higher in FM patients compared with those in MM (Figure 1D). Uncontrolled GVHD was the cause of 6 MM patients of 9 (66.7%) who died because of TRM, whereas in FM patients, 3 of 15 (20.0%) died because of uncontrolled GVHD.

Our study suggested that macrophages are involved in a specific type of acute GVHD that tended to be systemic and refractory to conventional therapies, such as corticosteroids or calcineurin inhibitors.[11-13] Differences in treatment efficacy could be explained by the difference in infiltrating cell types. Although efforts have been made at predicting refractory GVHD,[14-17] no confirmed factor has been established to date. Our findings could prove to be a relatively simple and useful method directly related to the prognosis of patients.

Macrophages could not be completely suppressed by current therapies for acute GVHD mainly targeting T cells. Considered together with

Table 2. Analyses of predictive factors for refractory GVHD in all 104 patients

Parameter	Odds ratio (95% CI)	P
More than 50 y old	1.21 (0.35-4.19)	.76
High disease risk	1.29 (0.44-3.76)	.65
Graft PB (vs BM)	1.19 (0.23-6.11)	.83
Unrelated donor	0.91 (0.30-2.73)	.86
HLA mismatch	1.96 (0.66-5.84)	.23
Conventional regimens	0.94 (0.27-3.23)	.92
Skin stage 3 or 4 at biopsy	1.97 (0.69-5.68)	.21
MT (> 100 $CD8^+$ cells)	1.26 (0.37-4.27)	.71
MM (> 200 $CD163^+$ cells)	3.79 (1.22-11.8)	.02

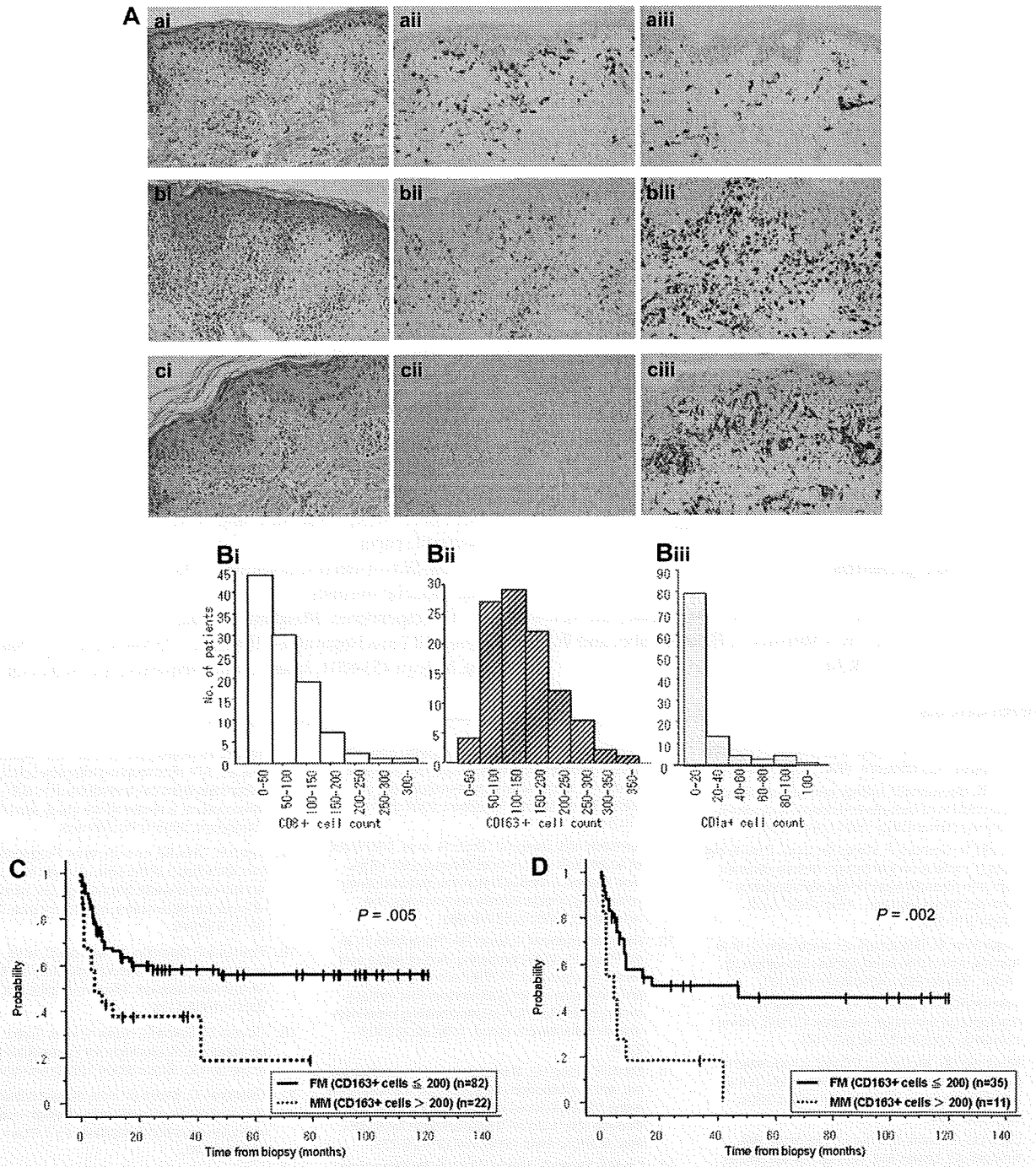

Figure 1. Skin biopsy specimens, infiltrating cells, and overall survival. Immunohistochemical analysis of representative skin biopsy specimen (A), the cell count distribution of $CD8^+$, $CD163^+$, and $CD1a^+$ cells (B), and the impact of MM on OS (C-D). (A) Tissue sections of skin biopsy were stained with hematoxylin and eosin (ai,bi,ci), or antibodies to $CD8^+$ (aii, bii, cii), or $CD163^+$ (aiii, biii, ciii) as detailed in "Methods." Shown are representative specimens of an MT/FM patient (ai-iii), a MT/MM patient (bi-iii), and an FT/MM patient (ci-iii). Original magnifications ×200. (B) Distribution of infiltrating cell counts (Bi, $CD8^+$; Bii, CD163; and Biii, CD1a). (C) OS according to $CD163^+$ cell counts (≤ 200 [FM] vs > 200 [MM]) in all patients. OS of patients with MM was significantly lower than that of those with FM (FM: 66.2% ± 10.6% at 1 year and 58.3% ± 11.4% at 3 years, MM: 37.8% ± 21.0% at 1 year and 37.8% ± 21.0% at 3 years, respectively; $P = .005$). (D) OS according to $CD163^+$ cell counts (≤ 200 vs > 200) in 46 patients undergoing steroid treatments. OS of patients with MM was significantly lower than that of those with FM (FM: 57.7% ± 17.1% at 1 year and 50.7% ± 17.4% at 3 years; MM: 18.2% ± 22.7% at 1 year and 18.2% ± 22.7% at 3 years, respectively; $P = .002$).

the fact that skin biopsies can be performed safely without any critical complications, our results support the importance of conducting skin biopsies of posttransplantation skin lesions. In cases where macrophage-dominant infiltration is observed in a skin biopsy specimen, macrophage-targeted therapies[18-23] could provide a clue to refractory GVHD.

In conclusion, macrophage infiltration of skin lesions after allo-SCT was shown to be a significant predictive factor for

Table 3. Analyses of risk factors for OS in all 104 patients

	Univariate		Multivariate	
Parameter	Hazard ratio (95% CI)	*P*	Hazard ratio (95% CI)	*P*
Older than 50 y	2.27 (1.23-4.20)	.009	—	—
High disease risk	1.87 (1.03-3.40)	.04	1.92 (1.06-3.50)	.03
Graft PB (vs BM)	2.04 (0.91-4.61)	.08	—	—
Unrelated donor	0.71 (0.40-1.29)	.26	—	—
HLA mismatch	1.13 (0.61-2.10)	.70	—	—
Conventional regimens	0.74 (0.39-1.39)	.35	—	—
Skin stage 3 or 4 at biopsy	1.11 (0.57-2.15)	.76	—	—
MT (> 100 $CD8^+$ cells)	1.10 (0.59-2.08)	.76	—	—
MM (> 200 $CD163^+$ cells)	2.38 (1.27-4.49)	.006	2.45 (1.30-4.61)	.006

— indicates not applicable.

refractory GVHD, as well as being a negative prognostic factor for OS. Our results indicate the importance of skin biopsies after allo-SCT and suggest the possibility of developing infiltrating cell-based strategies.

Acknowledgments

This study was supported in part by the Japan Leukemia Research Fund (S.N.) and in part by a Ministry of Health, Labor and Welfare of Japan Grant-in-Aid (K.M.).

Authorship

Contribution: S.N., S.T., M.I., and K.M. designed the research; S.N., S.T., and M.I. analyzed and interpreted the data; S.N. and S.T. performed statistical analysis; and S.N., T.G., A.S., K.W., M.Y., N.I., S.T., M.S., Y.O., M.I., and K.M. collected clinical data and wrote the paper.

Conflict-of-interest disclosure: The authors declare no competing financial interests.

Correspondence: Masafumi Ito, Department of Hematology, Japanese Red Cross Nagoya First Hospital, 3-35 Michishita-cho, Nakamura-ku, Nagoya 453-8511, Japan; e-mail: itom@nagoya-1st.jrc.or.jp.

References

1. Gordon S. The role of the macrophage in immune regulation. *Res Immunol.* 1998;149(7):685-688.
2. Stoy N. Macrophage biology and pathobiology in the evolution of immune responses: a functional analysis. *Pathobiology.* 2001;69(4):179-211.
3. Haniffa M, Ginhoux F, Wang XN, et al. Differential rates of replacement of human dermal dendritic cells and macrophages during hematopoietic stem cell transplantation. *J Exp Med.* 2009; 206(2):371-385.
4. Kristiansen M, Graversen JH, Jacobsen C, et al. Identification of the haemoglobin scavenger receptor. *Nature.* 2001;409(6817):198-201.
5. Fabriek BO, Dijkstra CD, van den Berg TK. The macrophage scavenger receptor CD163. *Immunobiology.* 2005;210(2-4):153-160.
6. Moestrup SK, Moller HJ. CD163: a regulated hemoglobin scavenger receptor with a role in the anti-inflammatory response. *Ann Med.* 2004; 36(5):347-354.
7. Zaba LC, Fuentes-Duculan J, Steinman RM, Krueger JG, Lowes MA. Normal human dermis contains distinct populations of $CD11c^+BDCA\text{-}1^+$ dendritic cells and $CD163^+FXIIIA^+$ macrophages. *J Clin Invest.* 2007;117(9):2517-2525.
8. Przepiorka D, Weisdorf D, Martin P, et al. 1994 Consensus Conference on Acute GVHD Grading. *Bone Marrow Transplant.* 1995;15(6):825-828.
9. Inamoto Y, Ito M, Suzuki R, et al. Clinicopathological manifestations and treatment of intestinal transplant-associated microangiopathy. *Bone Marrow Transplant.* 2009;44(1):43-49.
10. Nishida T, Hamaguchi M, Hirabayashi N, et al. Intestinal thrombotic microangiopathy after allogeneic bone marrow transplantation: a clinical imitator of acute enteric graft-versus-host disease. *Bone Marrow Transplant.* 2004;33(11): 1143-1150.
11. Kennedy MS, Deeg HJ, Storb R, et al. Treatment of acute graft-versus-host disease after allogeneic marrow transplantation: randomized study comparing corticosteroids and cyclosporine. *Am J Med.* 1985;78(6):978-983.
12. Ratanatharathorn V, Nash RA, Przepiorka D, et al. Phase III study comparing methotrexate and tacrolimus (prograf, FK506) with methotrexate and cyclosporine for graft-versus-host disease prophylaxis after HLA-identical sibling bone marrow transplantation. *Blood.* 1998;92(7):2303-2314.
13. Storb R, Deeg HJ, Whitehead J, et al. Methotrexate and cyclosporine compared with cyclosporine alone for prophylaxis of acute graft versus host disease after marrow transplantation for leukemia. *N Engl J Med.* 1986;314(12):729-735.
14. Lin MT, Storer B, Martin PJ, et al. Relation of an interleukin-10 promoter polymorphism to graft-versus-host disease and survival after hematopoietic-cell transplantation. *N Engl J Med.* 2003;349(23):2201-2210.
15. Sugimoto K, Murata M, Onizuka M, et al. Decreased risk of acute graft-versus-host disease following allogeneic hematopoietic stem cell transplantation in patients with the 5,10-methylenetetrahydrofolate reductase 677TT genotype. *Int J Hematol.* 2008;87(5):451-458.
16. Remberger M, Mattsson J, Hassan Z, et al. Risk factors for acute graft-versus-host disease grades II-IV after reduced intensity conditioning allogeneic stem cell transplantation with unrelated donors: a single centre study. *Bone Marrow Transplant.* 2008;41(4):399-405.
17. Lee KH, Choi SJ, Lee JH, et al. Prognostic factors identifiable at the time of onset of acute graft-versus-host disease after allogeneic hematopoietic cell transplantation. *Haematologica.* 2005; 90(7):939-948.
18. Patriarca F, Sperotto A, Damiani D, et al. Infliximab treatment for steroid-refractory acute graft-versus-host disease. *Haematologica.* 2004; 89(11):1352-1359.
19. Couriel D, Saliba R, Hicks K, et al. Tumor necrosis factor-alpha blockade for the treatment of acute GVHD. *Blood.* 2004;104(3):649-654.
20. Oussoren C, Storm G. Role of macrophages in the localisation of liposomes in lymph nodes after subcutaneous administration. *Int J Pharm.* 1999; 183(1):37-41.
21. Van Rooijen N, Sanders A. Liposome mediated depletion of macrophages: mechanism of action, preparation of liposomes and applications. *J Immunol Methods.* 1994;174(1):83-93.
22. Liu Q, Hamblin MR. Macrophage-targeted photodynamic therapy: scavenger receptor expression and activation state. *Int J Immunopathol Pharmacol.* 2005;18(3):391-402.
23. Demidova TN, Hamblin MR. Macrophage-targeted photodynamic therapy. *Int J Immunopathol Pharmacol.* 2004;17(2):117-126.

ARTICLES

Developmental and species-divergent globin switching are driven by BCL11A

Vijay G. Sankaran[1]*, Jian Xu[1,2]*, Tobias Ragoczy[3], Gregory C. Ippolito[4], Carl R. Walkley[1]†, Shanna D. Maika[4], Yuko Fujiwara[1,2], Masafumi Ito[5], Mark Groudine[3,6], M. A. Bender[3,7], Philip W. Tucker[4] & Stuart H. Orkin[1,2]

The contribution of changes in *cis*-regulatory elements or *trans*-acting factors to interspecies differences in gene expression is not well understood. The mammalian β-globin loci have served as a model for gene regulation during development. Transgenic mice containing the human β-globin locus, consisting of the linked embryonic (ε), fetal (γ) and adult (β) genes, have been used as a system to investigate the temporal switch from fetal to adult haemoglobin, as occurs in humans. Here we show that the human γ-globin (*HBG*) genes in these mice behave as murine embryonic globin genes, revealing a limitation of the model and demonstrating that critical differences in the *trans*-acting milieu have arisen during mammalian evolution. We show that the expression of BCL11A, a repressor of human γ-globin expression identified by genome-wide association studies, differs between mouse and human. Developmental silencing of the mouse embryonic globin and human γ-globin genes fails to occur in mice in the absence of BCL11A. Thus, BCL11A is a critical mediator of species-divergent globin switching. By comparing the ontogeny of β-globin gene regulation in mice and humans, we have shown that alterations in the expression of a *trans*-acting factor constitute a critical driver of gene expression changes during evolution.

The extent to which changes in *cis*-regulatory elements or the *trans*-acting environment account for differences in gene expression in closely related species is the subject of debate[1,2]. Some studies suggest that changes in *cis*-regulatory elements are largely responsible for many interspecies differences in gene expression[3,4]. The contribution of alterations in the *trans*-acting milieu is less established. With their temporal switches of globin expression, mammalian β-globin loci serve as a model for developmental gene regulation[5]. To study the regulation of human *cis*-elements in a mouse *trans*-acting environment, we used human β-globin locus transgenic mice (β-locus mice). The regulation of the human β-globin locus has been widely studied using such mouse models[6–8]. It is generally accepted that these mice provide a valid system for evaluating human developmental globin gene regulation, although some differences have been noted between humans and these mice. For example, the onset of γ-globin expression occurs during the embryonic, yolk sac stage of erythropoiesis in the mouse, whereas high-level expression of this gene occurs during the fetal liver stage in man. Moreover, the switch from γ-globin to adult β-globin occurs during early fetal liver erythropoiesis in these mice[6–8], whereas it occurs around the time of birth in humans[9]. Furthermore, differences have been noted in the capacity of the mice to respond to fetal haemoglobin (HbF)-eliciting responses that are active in humans[10,11]. We began by evaluating whether these mice respond to stimuli that consistently increase the level of HbF in humans[12]. We found that these mice have much lower basal levels of γ-globin expression than adult humans, and fail to respond to stimuli that result in increased levels of HbF in humans (Supplementary Fig. 1). Also, in a model of juvenile myelomonocytic leukaemia created in these mice, no increase in γ-globin levels was observed, in contrast to the high levels of γ-globin seen in humans with this syndrome[13].

Human fetal globin genes behave as mouse embryonic genes

To pursue the underlying basis of these species differences, we re-assessed the ontogeny of human γ-globin expression during mouse development. First we isolated circulating blood from embryos at a time when γ-globin expression is observed (embryonic day (E)13.5)[6–8]. Using differences in cell size that permit the separation of circulating primitive and definitive lineage cells using flow cytometry[14,15], we enriched the erythroid cells in blood from E13.5 β-locus mice (Fig. 1a). As anticipated, the expression of the mouse embryonic gene εy globin (*Hbb-y*)—a gene confined to the primitive erythroid lineage along with mouse βh1 globin (*Hbb-bh1*)[14,15]—was enriched (approximately fivefold) in the primitive population relative to the definitive population (Fig. 1b). Consistent with this distribution, human embryonic ε-globin (*HBE*, also known as *HBE1*) transcripts were similarly enriched in the primitive population (Fig. 1b). Surprisingly, no difference was observed between the relative enrichment of the embryonic genes and the degree of enrichment of human γ-globin transcripts in the primitive erythroid population compared to the definitive cells (Fig. 1b). This finding indicates that the human γ-globin genes are not robustly expressed in early definitive erythroid cells in β-locus mice.

We then used immunohistochemistry (IHC) of γ-globin in E13.5 embryos to examine its cellular distribution. IHC of human fetal liver showed positive labelling of all erythroblasts (Fig. 1c). In contrast, most of the erythroblasts present in the murine fetal liver of β-locus mice failed to stain for γ-globin. We observed occasional large nucleated, megaloblastic cells in fetal liver positive for γ-globin (Fig. 1d, e). Morphologically these cells resemble primitive cells that continue to circulate in substantial numbers during this period of gestation[5]. Consistent with this interpretation, the numerous γ-globin-positive cells seen in the circulation were all megaloblastic primitive cells,

[1]Division of Hematology/Oncology, Children's Hospital Boston and Department of Pediatric Oncology, Dana-Farber Cancer Institute, Harvard Stem Cell Institute, Harvard Medical School, Boston, Massachusetts 02115, USA. [2]Howard Hughes Medical Institute, Boston, Massachusetts 02115, USA. [3]Fred Hutchinson Cancer Research Center, Seattle, Washington 98109, USA. [4]Institute for Cellular and Molecular Biology, The University of Texas at Austin, Austin, Texas 78712, USA. [5]Department of Pathology, Japanese Red Cross, Nagoya First Hospital, Nagoya, Japan. [6]Department of Radiation Oncology, and [7]Department of Pediatrics, University of Washington, Seattle, Washington 98195, USA. †Present address: St Vincent's Institute of Medical Research, Fitzroy, Victoria 3065, Australia.
*These authors contributed equally to this work.

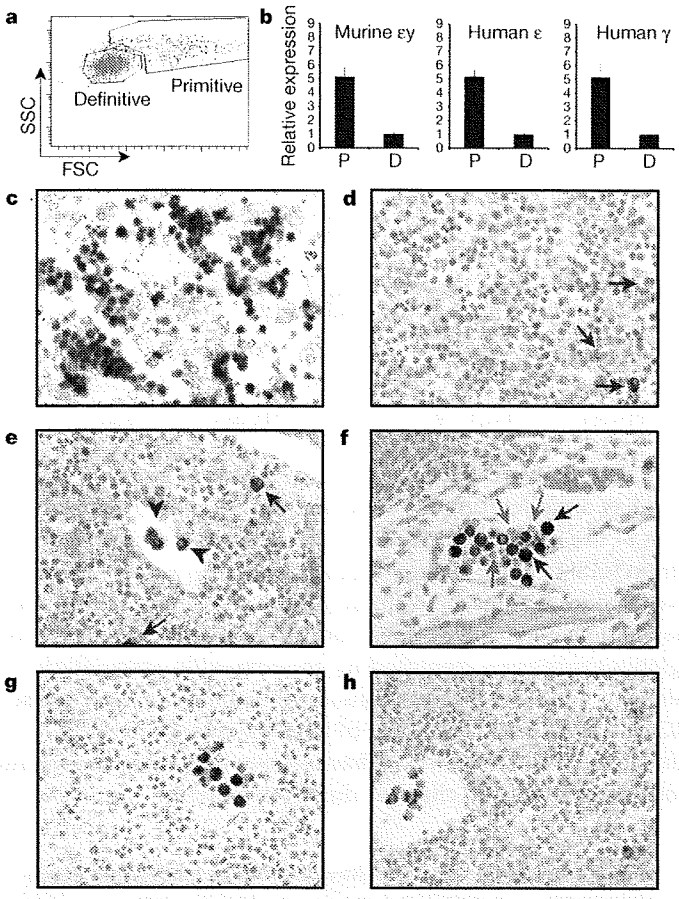

Figure 1 | Human γ-globin is primarily expressed in primitive erythroid cells of β-locus mice. **a**, Representative FACS plot showing forward light scatter (FSC; linear scale) versus side scatter (SSC; log scale) for E13.5 embryonic blood. Gating is shown to allow for the enrichment of primitive (blue population) and definitive (red population) lineages. **b**, The relative expression of the murine εy globin gene, human embryonic ε gene and human γ-globin genes showed similar relative enrichment levels in the primitive population (P) as compared with the definitive population (D). Results are shown as mean and s.d. ($n \geq 3$ per group). $P = 0.98$ for a two-sided *t*-test comparing the relative enrichment of εy with γ-globin. **c–h**, Representative IHC staining with an anti-HbF antibody from human and murine E13.5 fetal livers. All images are taken with a ×60 objective. **c**, Human fetal livers contain numerous erythroblasts, which all stain positive for γ-globin expression. **d, e**, In contrast, murine fetal liver definitive erythroblasts do not show major γ-globin staining and only occasional cells with megaloblastic primitive morphology show staining (blue arrows). **e, f**, Many megaloblastic primitive cells in the circulation show highly positive staining (**e**, blue arrowheads; **f**, blue arrows), whereas smaller definitive erythrocytes are negative (**f**, red arrows). **g, h**, Staining performed on the single copy YAC lines A20 and A85 (ref. 8) showed similar staining patterns. Positive staining was determined in comparison with background staining from transgene-negative littermate controls.

whereas enucleate, smaller definitive cells were uniformly negative (Fig. 1e, f). To generalize these findings, we performed similar immunohistochemical staining in other independently derived lines of β-locus mice (Fig. 1g, h)[8]. In all lines, γ-globin expression (as indicated by positive IHC) was confined to circulating megaloblastic cells that were infrequent in fetal liver parenchyma. Because similar observations have been made in independently derived β-locus mice, our findings demonstrate a characteristic feature of β-locus mice.

Divergent behaviour of human β-globin loci in mice

To gain further insight at the single-cell level, we used primary transcript RNA fluorescence *in situ* hybridization (PT-FISH) to examine the relative expression of the endogenous mouse and human globin genes at different stages of ontogeny[16,17]. First, we examined the relative expression of human γ- and β-globin (with murine α-globin as a control) in E11.5 primitive erythroid cells from two independent transgenic lines (A20 and A85). Consistent with previous analyses demonstrating high-level expression of γ-globin at the primitive erythroid stage in β-locus mice, we noted relatively high expression of γ-globin by PT-FISH, with low or absent expression of human β-globin (Fig. 2a, b). Among circulating primitive cells from a later stage of development (E13.5) a similar pattern was observed, although more human β-globin expression was seen and an overall reduction in the percentage of cells with a PT-FISH signal (using the murine α-globin control) was noted, with only a fraction of the cells (~one-third) showing transcriptionally active loci at a single time point (Fig. 2a, b). Examples of the cells used in this analysis are shown (Fig. 2e–g). An interesting observation made with concomitant PT-FISH analysis of human γ- and β-globin is the extent of cotranscription, which represents the concomitant presence of two primary transcript signals in the same gene locus (Supplementary Fig. 2 and Supplementary Information).

Comparison of mouse embryonic εy globin with γ-globin showed similar expression levels of the mouse embryonic gene with the human γ-globin in circulating primitive cells from E13.5 (Fig. 2c,

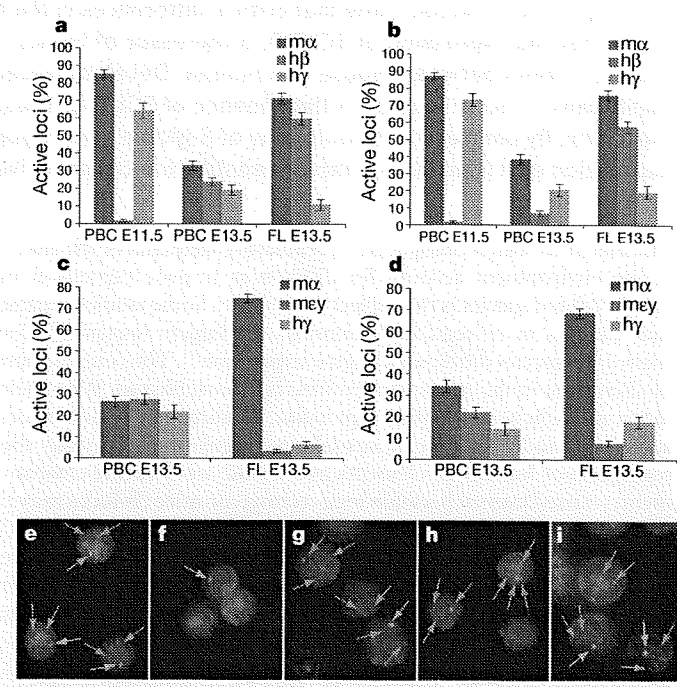

Figure 2 | PT-FISH analysis shows that γ-globin expression parallels the murine embryonic globins in primitive erythroid cells. **a–d**, Two independent lines of transgenic YAC mice, A85 (**a**, **c**) and A20 (**b**, **d**), were analysed using four-colour PT-FISH. For the first set of experiments, probes were made to target murine α-globin (mα), human β-globin (hβ) and human γ-globin (hγ). Additionally, 4,6-diamidino-2-phenylindole (DAPI) was used to identify nuclei of cells. Error bars denote the s.d. **a**, **b**, The expression of γ-globin predominates within the two lines in the primitive populations seen circulating in primitive blood cells (PBC) from embryos E11.5 and E13.5. Minor expression is seen in the mature definitive populations from fetal liver (FL) at E13.5. Many of these cells may represent primitive cells found in the fetal liver parenchyma. **c**, **d**, Probes were made to target murine α-globin (mα), murine εy globin (mεy) and human γ-globin (hγ). These data show parallel expression of mεy and hγ. **e–g**, Representative images with the staining pattern of **a** and **b** at each developmental time point are shown for PBC at E11.5 (**e**), at E13.5 (**f**), and fetal liver at E13.5 (**g**). **h, i**, Representative images with the staining pattern of **c** and **d** are shown for PBC at E13.5 (**h**) and fetal liver at E13.5 (**i**). The colour of the bars in all graphs (and arrows in images) corresponds to the colours of the probes that were detected for each of these primary transcripts. The graphs depict the percentage of active loci and are measured for ≥100 nuclei per probe set at each time point. Original magnification, ×100.

d, h, i). This finding indicates that the expression of the human γ-globin genes parallels that of the mouse embryonic β-like genes in the mouse *trans*-acting environment. Fetal liver cells from E13.5 were analysed in a similar manner, by examining the expression of mouse εy and human γ-globin by PT-FISH in these cells. Only a low percentage of cells showed staining for either εy or γ-globin (Fig. 2c, d), compared with robust transcription of human β-globin at the same stage (Fig. 2a, b). Consistent with previous developmental analyses in mice[14,17], cells positive for mouse εy represent circulating primitive cells present in the mouse fetal liver. The cells that are positive for human γ-globin expression are also likely to be primitive erythroid cells, and it is important to recognize that in these cells only a fraction (~one-third) of loci are active at any single time point, thereby limiting the degree of concomitant expression seen. Of note, 45% and 54% (in the A85 and A20 lines, respectively) of the primitive cells from E13.5 with γ-globin transcript showed expression of εy globin, supporting the notion that γ-globin is treated as an embryonic gene in the mouse *trans*-acting environment. Interestingly, an early analysis of very low expressing transgenes lacking critical locus region regulatory sequences had suggested that γ-globin indeed behaved as an embryonic gene, as we have shown for mice containing the entire robustly expressed human β-locus[18].

BCL11A restricts mouse embryonic β-like globin expression

From these results we conclude that the homologous mouse erythroid *trans*-acting environment differs from that of the human, presumably with respect to the composition or regulation of critical transcriptional regulators. We have recently shown that the gene *BCL11A*, which contains genetic variants that affect HbF levels in humans[19–22], encodes a developmental-stage-specific repressor of the human γ-globin genes[23]. Our previous findings were confined to an analysis of human erythroid cells, in which we found that full-length forms of BCL11A were expressed robustly in adult bone marrow erythroblasts, at substantially lower levels in fetal liver, and were absent in primitive erythroblasts. Moreover, shorter variant forms of BCL11A are expressed in human primitive and fetal liver erythroblasts, both of which express γ-globin. To investigate potential species differences in BCL11A protein expression, we examined stage-matched populations of mouse and human erythroid cells that were subjected to fluorescence-activated cell sorting (FACS). Remarkably, comparison of BCL11A expression in mouse and human samples shows notable differences (Fig. 3a and Supplementary Fig. 3). First, BCL11A protein and RNA transcripts are absent in primitive erythroid cells of mice. Second, full-length BCL11A forms are expressed at similar levels in definitive erythroid cells of both mouse fetal liver and bone marrow, whereas no shorter variant forms could be identified in mice (Fig. 3a). These results highlight important interspecies differences that could potentially have a role in mediating divergent globin gene regulation. A model on the basis of our findings of the developmental expression of the β-like globin genes in humans, mice and β-locus mice is shown, along with a summary of BCL11A expression in these two species (Fig. 3b).

We have demonstrated that the expression of the human γ-globin genes strictly parallels that of the mouse embryonic genes, εy and βh1, in the context of the mouse *trans*-acting environment. Moreover, the pattern of BCL11A expression suggests a role throughout definitive erythropoiesis in mice, as opposed to its predominant role after birth in humans. Thus, we propose that changes in BCL11A expression may be responsible, at least in part, for the observed interspecies divergent expression of β-like globin genes. To test directly a potential role for BCL11A in silencing the endogenous embryonic genes in the definitive erythroid lineage, we examined BCL11A knockout mice. As described previously[24], *Bcl11a*$^{-/-}$ mice die in the perinatal period from unknown causes. We examined *Bcl11a*$^{-/-}$ mice at E14.5 and E18.5 during gestation when robust definitive erythropoiesis is taking place in the fetal liver (Supplementary Fig. 4). By phenotypic and morphological approaches[25,26], erythropoiesis appeared ostensibly

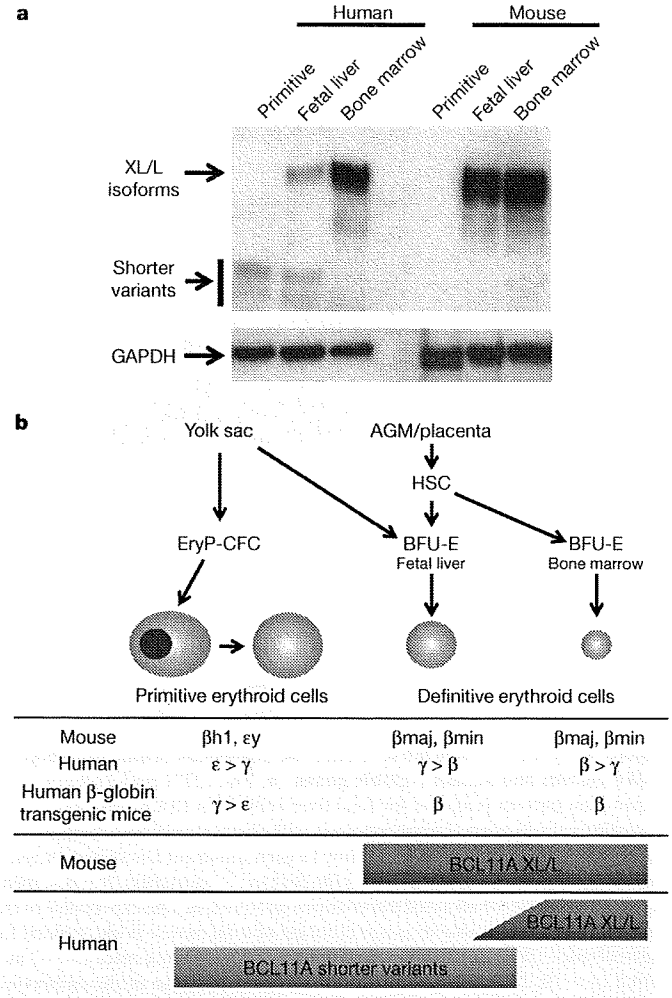

Figure 3 | BCL11A expression varies between humans and mice, suggesting a model for *trans*-acting variation in β-globin gene expression. a, In human cells full-length proteins of BCL11A (XL/L, full-length isoforms[23]) are reduced in cell populations that express high levels of γ-globin, including primitive and fetal liver cells[23]. Furthermore, short variant forms are present at these earlier developmental stages. All human cells were sorted for CD235 and CD71 expression. In contrast, in murine cells, full-length BCL11A protein expression is evident in all definitive progenitor populations, including sorted stage-matched E13.5 fetal liver and bone marrow erythroid cells (all populations were sorted for TER119$^+$ (also known as LY76) and CD71$^+$ (also known as TFRC)). No expression of BCL11A in murine primitive cell populations was detected. **b,** This model summarizes the ontogeny of β-like globin gene regulation in humans, mice and β-locus mice[5,9]. The ontogeny of mammalian erythropoiesis and progenitor populations is shown at the top. Progenitor populations, including primitive erythroid populations (EryP-CFC), definitive haematopoietic stem cells (HSC), and definitive erythroid burst-forming unit cells (BFU-E) are depicted. The aorto-gonado-mesonephros (AGM) and the placenta are sites of definitive haematopoiesis. The patterns of β-like globin and BCL11A expression seen in the two species are shown below.

normal in these embryos (Fig. 4a and Supplementary Figs 5–7). We then assessed expression of the mouse globin genes. In strong support of our hypothesis, we observed that silencing of the expression of mouse embryonic globin genes fails to occur in E14.5 and E18.5 fetal liver erythroid cells (Fig. 4b–e and Supplementary Fig. 8). Restriction of embryonic globin expression to the primitive lineage is lost. Expression of the εy and βh1 globin genes was upregulated by 70- and 350-fold, respectively, at E14.5 (Fig. 4b). Together, these embryonic globin genes account for 50% of the total β-like globin genes at this stage, compared with 0.4% in the controls. At E18.5, whereas the contribution of their transcripts to total β-like globin transcripts was reduced, εy and βh1 globin transcripts were increased